Department of Biomedical Sciences
Of the Veterinary University of Vienna

Institute for Medical Biochemistry

Impact of Transplanting LSK Cells with a CRISPR/Cas9 Induced EVI2A KO into Mice

Master Thesis

Veterinary University Vienna

By: Helene Foissner

Heidelberg, 14.12.2022

Declaration of Authenticity

“As author and creator of this work to hand, I confirm with my signature knowledge of the relevant copyright regulations.

I hereby declare that I completed the present work independently and that any ideas, whether written by others or by myself, have been fully sourced and referenced. I am aware of any consequences I may face on the part of the degree program director if there should be evidence of missing autonomy and independence or evidence of any intent to fraudulently achieve a pass mark for this.

I further declare that up to this date I have not published the work to hand nor have I presented it to another examination board in the same or similar form. I affirm that the version submitted matches the version in the upload tool.”

Examiner: Prof. Dr. Florian Grebien
Institute: Veterinary University Vienna

Place, Date

Signature

Acknowledgements

Throughout my internship at DKZ I received great support from many people I would like to thank herein.

First and foremost, I want to thank **Dr. Michael Milsom** for having me in the lab and providing supervision. Thank you giving me the opportunity to learn from your experience, I am happy to have worked for your amazing research.

Of course, great thanks to **Theo Aurich**, for both supervision and support. We had a lot of fun in the lab, even when nothing seemed to work. You supported and appreciated input from me and helped me carry on. Also, I believe we both benefited from working together, and I hope you enjoyed our time in the lab as much as I did.

Without the help of my colleagues in the Milsom lab, the time would not have been the same. Thank you for scientific (and personal) support: **Esther Rodrígues Correa**, **, Dr. Jeyan Jayarajan, Melanie Ball, Ian Ghezzi, Foteini Fotopoulou, Viktoria Flore, Dr. Charles Dussiau, Lena Bognar and Dr. Susanne Lux**. I really appreciated having all of you to chat about science, discussing results and having someone to ask questions to.

Special thanks to **Melanie Ball** for all kinds of support and making all live so much easier in the lab. And to **Esther Rodríguez Correa** for proofreading on the one hand and supporting me in my scientific development.

Apart for the lab, I also want to thank **Manuel Ronceros-Möhring** and **Valerie Christ** for not only proofreading my thesis, but also supporting me in the writing process. Also, thanks to my WG, **Anna Weigelt**, **Antonia Jäcklin**, **Amir Tabar and Manuel Ronceros-Möhring** for providing me with a new home during my time in Heidelberg. And thanks to **Anna Krannich** for always being there for me, irrespective of distance.

Kurzfassung

Hämatopoese ist ein hoch regulierter Prozess, um die Balance der verschiedenen hämatopoetischen Zellen zu gewährleisten. Jeder Zelltyp wird über eine bestimmte Genexpressions-Landschaft definiert, die sich im Laufe der Differenzierung von hämatopoetischen Stammzellen zu ausgereiften Zellen variiert. In Krankheitsbildern wie zum Beispiel Leukämien, kann eine fehlregulierte Genexpression von bestimmten Proteinen zu einer Vermehrung oder Verlust von einzelnen Subtypen führen. Studien, die zuvor von unserer Gruppe durchgeführt wurden, haben festgestellt, dass Evi2a eine essenzielle Rolle in der Spezifikation von definitiven hämatopoetischen Stamm- und Vorläufer Zellen während der Embryogenese spielt. Abgesehen davon ist bisher wenig über das Transmembranprotein Evi2a bekannt. Das Ziel der folgenden Studie ist daher den Einfluss von Evi2a auf die adulte Hämatopoese *in vivo* zu testen. Dafür wurde ein CRISPR/Cas9 System entwickelt, um Evi2a mit Hilfe von lentiviraler Transduktion auszuknocken. Um den Knockout auf genomischer und transkriptomischer Ebene zu validieren, wurden zusätzlich murine Fibroblasten und murinen Zellelinien für Akute Myeloide Leukämie transduziert und sequenziert. Daraufhin wurden murine Lin- Sca1+ cKit+ (LSK) Zellen isoliert und ebenfalls *in vitro* transduziert. Diese wurden das *in vitro* auf das Potenzial zur Kolonie Formation getestet und in Empfängermäuse transplantiert. Sowohl der Spenderchimerismus also auch B Zellen, T Zellen und myeloide Zellpopulationen wurden im peripheren Blut in 4-Wochen Intervallen analysiert. Die Zellen wurden mit anhand von Durchflusscytometrie analysiert und anschließend sortiert, um festzustellen, ob der *evi2a* Genelokus eine Läsion aufweist. Die bisher gesammelten Daten lassen vermuten, dass der Evi2a Knockout keinen Einfluss auf die hämatopoetische Differenzierung hat, es ist jedoch notwendig noch weitere Zeitpunkte zu analysiere. Neben der Evaluierung eines Effekts von Evi2a in der Hämatopoese, konnten wir ein Protokoll etablieren, um ein Gen nach Wahl in LSK Zellen auszuknocken und zu Zellen anschließend zu transplantieren. In Zukunft wird dieses Protokoll angewendet werden können, um Genfunktionen *in vivo* zu testen, ohne die kostspielige und zeitintensive Erschaffen von neuen Transgenen Mauslinien.

Abstract

Hematopoiesis is a highly regulated process to maintain a balance of the different hematopoietic cells. Each subset is defined by a particular gene expression landscape that varies throughout differentiation from a hematopoietic stem cell (HSC) to a mature cell. Upon diseases such as cancer, deregulated expression of certain proteins can lead to an expansion or loss of individual subsets. Previous studies by our group have identified Evi2a to be essential to the specification of definitive hematopoietic stem and precursor cells (HSPCs) during embryonic development. Besides this, little is known about the supposed transmembrane protein Evi2a. In the following study, we therefore set out to investigate the influence of Evi2a on adult hematopoietic differentiation *in vivo*. To achieve this, a CRISPR/Cas9 system was developed to knock out (KO) Evi2a using a lentiviral vector. Successful KO was validated in murine fibroblastic and acute myeloid leukemia (AML) cell lines on a genomic and transcriptomic level. Afterwards, murine Lin- Sca1+ cKit+ (LSK) cells were isolated and transduced *in vitro*. Using these, i*n vitro* colony forming unit (CFU) potential was assessed and cells were transplanted into recipient animals. Donor chimerism, as well as B cell, T cell and myeloid cell populations in the peripheral blood were analyzed in 4-week intervals. Next to flow cytometric analysis, cells were sorted to determine the presence of a genetic lesion at the *evi2a* locus in the differentiated populations. The preliminary data collected so far indicates no impairment of hematopoietic differentiation upon KO of Evi2a, but further timepoints will have to be analyzed. Besides evaluating the effect of an Evi2a KO on hematopoiesis, we established a new protocol for creating a gene KO in LSK cells and subsequent transplantation. In the future, this will enable studies of gene functions *in vivo* without the costly and time-consuming process of creating new transgenic mouse lines.

Keywords: Hematopoiesis, CHRISPR/Cas9, Bone marrow transplantation, EVI2A

Table of Contents

List of Abbreviations

A	
Ab	Antibody
AML	Acute Myeloid Leukemia
B	
BM	Bone Marrow
BMT	B-, T- and myeloid cells
bp	Base pair
C	
CD	Cluster of differentiation
CFU	Colony Forming Unit
CLP	Common lymphoid progenitor
CMP	Common myeloid progenitor
CRISPR	Clustered Regularly Interspaced Short Palindromic Repeats
D	
ddH_2O	Demineralized Water
DMEM	Dulbecco's Modified Eagle Medium
E	
EDTA	Ethylenediamine tetraacetic acid
EoBP	Eosinophil-Basophil progenitor
Evi2a	Ectopic viral integration site 2A
F	
FACS	Fluorescence-activated cell sorting
FCS	Fetal calf serum
FSC	Forward scatter
G	
GMP	Granulocyte-monocyte progenitor
gRNA	Guide RNA
H	
HEK293T	Human embryonic kidney 293T

HSC	Hematopoietic stem cell
K	
KD	Knock-down
KO	Knock-out
L	
LMPP	Lymphoid-primed multipotential progenitor
LSK	Lin- Sca1+ cKit+
LT-HSC	Long-term hematopoietic stem cell
M	
MEP	Megakaryocytic-erythrocyte progenitor
MFI	Mean fluorescent intensity
MOI	Multiplicity of infection
MPP	Multipotent progenitor
N	
Nt	Non-targeting
P	
P/S	Penicillin and streptomycin
PB	Peripheral blood
PBS	Phosphate-buffered saline
PBMC	Peripheral blood monocytic cells
R	
rhEPO	Recombinant human erythropoietin
rhFLT3-L	Recombinant human
rmIL-3	Recombinant murine interleukin-3
rmIL-6	Recombinant murine interleukin-6
rmIL-7	Recombinant murine interleukin-7
rmIL-11	Recombinant murine interleukin-11
rmSCF	Recombinant murine stem cell factor
rmTPO	Recombinant murine thrombopoietin
RPMI	Roswell Park Memorial Institute

RT	Room Temperature
S	
Sca-1	Stem cell antigen 1
scCFU	Single cell colony forming unit
SFEM	Serum Free Expansion Medium
SSC	Sideward scatter
T	
TBI	Total body irradiation
TPM	Transcripts per million
TU	Transducing Units
W	
WT	Wild type

Introduction

1.1 Hematopoietic system

Blood has multiple functions, for instance providing organs with nutrients and oxygen or detecting and eliminating pathogens. To accomplish these versatile tasks, blood consists of different highly specialized cell types. In adult physiologic hematopoiesis, all blood cells arise from hematopoietic stem cells (HSC) residing in the bone marrow (BM) in a particular microenvironment, the niche. HSCs are defined by exhibiting the capacity to self-renew and differentiate into all hematopoietic cell types (multipotency). Consequently, mature cells do not show self-renewal and only have restricted or no differentiation capacities. Both mature and immature hematopoietic cell populations are usually characterized immunophenotypically, meaning by their expression of certain cell surface markers, for example CD8 for cytotoxic T cells. Throughout maturation, these expression profiles change, enabling the identification and isolation of defined cells via fluorescent activated cell sorting (FACS). A subset of immature hematopoietic cells in the BM express low or no lineage markers but do express stem cell antigen 1 (Sca-1) and cKit (CD117). These Lin-Sca-1+cKit+ (LSK) cells consist of HSCs (less than 10 %) and multipotent progenitors (MPPs) and are the basis for further hematopoietic differentiation [1] [2].

It has long been thought that hematopoiesis follows a stepwise hierarchical differentiation where long term HSCs are at the top of the hierarchy, directly followed by short term HSCs. These are distinguished by their repopulation capacities. HSC then differentiate into MPPs, that retain differentiation potential whilst self-renewal is reduced. MPPs then further branch into committed progenitor populations of common myeloid progenitors (CMPs) and lymphoid-primed multipotential progenitors (LMPPs), that then give rise to common lymphoid progenitors (CLPs) [3]. Both CMPs and LMPPs have the potential to finally differentiate into granulocyte/macrophage and lymphoid lineages [4]. CMPs may also give rise to erythrocytes, megakaryocytes, and platelets, whereas CLPs will rather differentiate into T and B cells, innate lymphoid cells and natural killer cells [3]. Notably, this scheme is widely characterized by previous studies applying bulk analysis of immunophenotypically defined cell populations [1], not emphasizing heterogeneity within these. Consequently, evidence for the hierarchical

differentiation is missing. Through advances in single cell technologies this dogma has been revised. *Brand and Morrisey (2020)* summarized recent findings challenging the classical hierarchical differentiation model, according to which committed progenitor cells can only give rise to a defined subset of progeny cells [5]. Further, single cell RNA sequencing has revealed a significant heterogeneity within immunophenotypically defined long-term HSCs, in terms of self-renewal and multipotency [4]. Therefore, a more flexible differentiation model has been suggested and is widely accepted now, shown in **Figure 1c**. Nonetheless, although the above-mentioned progenitors are not fully restricted to the according cells, hierarchical differentiation can be accepted for a more simplified depiction of basic dynamics of hematopoiesis. A visualization of simplified models versus a continuous model is depicted in **Figure 1**.

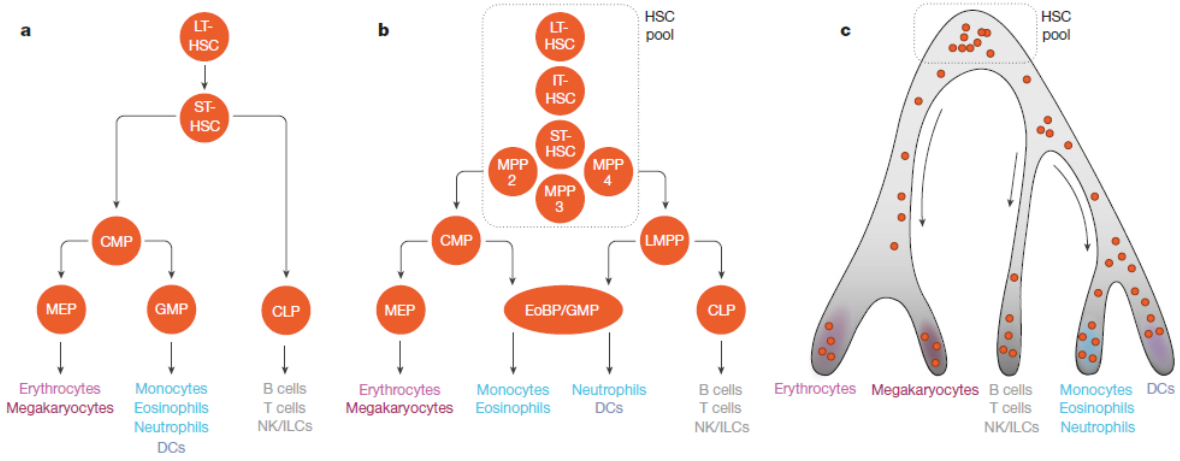

Figure 1: Timeline of development of hematopoiesis models. a) based on research around the year 2000 showing differentiation of long-term HSCs (LT-HSC) into short-term HSCs (ST-HSC), directly follwed by branching into CMPs, giving rise to megakaryocyte-erythrocyte progenitor (MEP) and granulocyte-monocyte progenitor (GMP), and CLPs, giving rise to all lymphoid cells. **b)** Depicts a more recent scheme including findings from 2005 until 2015: increased hetereogeneity of the HSC pool is emphasized including intermediate HSCs (IT-HSC) and divison of progenitors into eosionphil-basophil progenitor (EoBP) and GMPs. Transdifferntiation of LMPPs and GMPs is apreciated. **c)** Most recent view of hematopoietic tree, based on single cell transciptional data revealing the contiuous character of differentiation. The red dots indicate single cells that can be at any point of the continuum instead of any defined state, as indicated in a) and b) [3].

1.2 Hematopoietic stem cell transplantation

To study HSC function and potential, transplantation experiments in mice have been considered gold standard for the past years. These experiments are essential for understanding HSCs and remain the only method to date to prove self-renewal [3]. For HSC transplantation experiments, recipient mice are preconditioned via total body irradiation (TBI) or treatment with depleting antibodies to eliminate the preexisting hematopoietic cells. Donor cells are subsequently transplanted, often in combination with supportive BM to ensure animal survival. By transplanting different hematopoietic cell populations, the reconstitution and self-renewal capacities can be evaluated [4]. Previous transplantation studies have shown quick HSC response after TBI. Platelet production is evident only 7 – 9 days after the transplant. Followed by differentiation into the megakaryocyte, myeloid and lymphoid lineages in a stepwise manner, starting with myeloid lineages followed by T and B cells [6]. When transplanting bulk LSK cells or HSCs followed by continuous peripheral blood (PB) analysis, these temporal dynamics are evident [7]. However, in a single cell HSC transplant setting these dynamics are not observed, (temporal) differentiation outcome is mainly determined by a lineage bias of the transplanted cell [8].

Whether these observations are induced by a transplant setting, or also evident in normal hematopoiesis remains unclear, since dynamics in a non-transplant model are less studied due to technical constraints. Concordantly, the exact dynamics and validity of this stepwise differentiation model has yet to be fully understood [4] [9].

1.3 Ectopic viral integration site 2A (EVI2A)

In 1990, Buchberg et al. first described Evi2a and linked viral integration into this gene locus to increased incidence of myeloid leukemia in mice. They identified the gene by hybridization with unique sequence probes. Using northern analysis, they also showed that two different transcripts are present, whereas the bigger one of the two was less abundant. Further investigation of the genomic sequence and the predicted amino acid sequence revealed that no homologous gene is present in the data bases of EMBL, GEN-BANK or NBRF, suggesting that the Evi2 locus codes for a novel oncogene [10]. UniProt (https://www.uniprot.org/uniprotkb/P22794/entry#similar_proteins) and The Human Protein

Atlas (https://www.proteinatlas.org/ENSG00000126860-EVI2A) show that the predicted coding region contains structural motifs of a transmembrane protein. More specific, a single pass type I membrane protein that has a helical domain, flanked by 2 topological domains located on the extra- and intracellular region.

Interest to Evi2a was initiated by Paul Kaschutnig and Marleen Buechler two former PhD students from our group, who found that Evi2a is involved in embryogenesis. When knocking out Evi2a in embryonic stem cells *in vitr*o the formation of hematopoietic cells was impaired, and normal embryonic development of hematopoietic cells seems to be delayed (unpublished). This implied that Evi2a is important in epithelial to hematopoietic transition and raised the interest of Evi2a in hematopoiesis. In the adult human setting high expression levels especially in monocytes, interestingly however not in macrophages is evident, as depicted in **Figure 2 (**acquired from The Human Protein Atlas). Database research for mice using "genevisible" (https://genevisible.com/cell-types/MM/UniProt/P20934) revealed similar results. Expression profiles in mice resemble those in human, showing that Evi2a is conserved throughout species. Mouse experiments are therefore feasible to study the functional relevance of Evi2a.

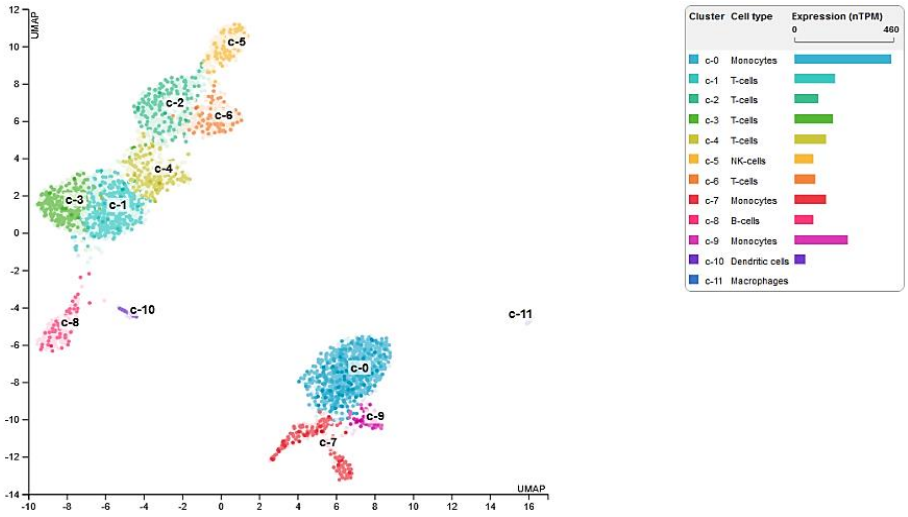

Figure 2: Database search for Evi2a protein shows UMAP of peripheral blood monocytic cells (PBMC) for Evi2a expression (TPM = transcripts per million)

1.4 Acute Myeloid Leukemia

AML is a hematopoietic malignancy that is characterized by abnormal clonal expansion of myeloid progenitor cells or progranulocytes in both, BM and PB. The disease is very heterogeneous, which makes the identification of appropriate treatment strategies particularly challenging. Although our understanding of the underlying biology is increasing steadily, treatment outcomes remain unsatisfying [11] [12]. AML subtypes can be classified via different classification schemes based on morphological or genetic features. Generally molecular and prognostic systems are now widely used for classification [13]. However previous database research, performed by Theo Aurich, revealed that Evi2a is upregulated in M4 and M5 subtypes of the French-American-British (FAB) classification (unpublished data). The FAB scheme relies on morphologic and cytochemical features, where M0 to M5 includes AMLs that involve myeloid blasts with increasing maturation [13]. The role of Evi2a in more mature subtypes of AML remains unclear and might be a result of maturation or might be causative for the expansion of mature myeloid populations.

Given the high Evi2a expression in monocytes, and the suggested role in hematopoiesis, Theo Aurich analyzed expression data in human AML cells lines. Depending on the cell line, expression is variable, it will therefore be interesting to compare driver mutations, disease prognosis, and response to treatment dependent on Evi2a. Theo Aurich also developed a pTripz knock down (KD) vector targeting human Evi2a mRNA, which was tested on MOLM-13, Set-2 and OCI-AML2 cells since expression levels range from highest to lowest. Compared to the empty vector no significant growth inhibition was detected in the co-culture assay of KD cells with non-transduced control cells (unpublished, **Figure 3b-d**).

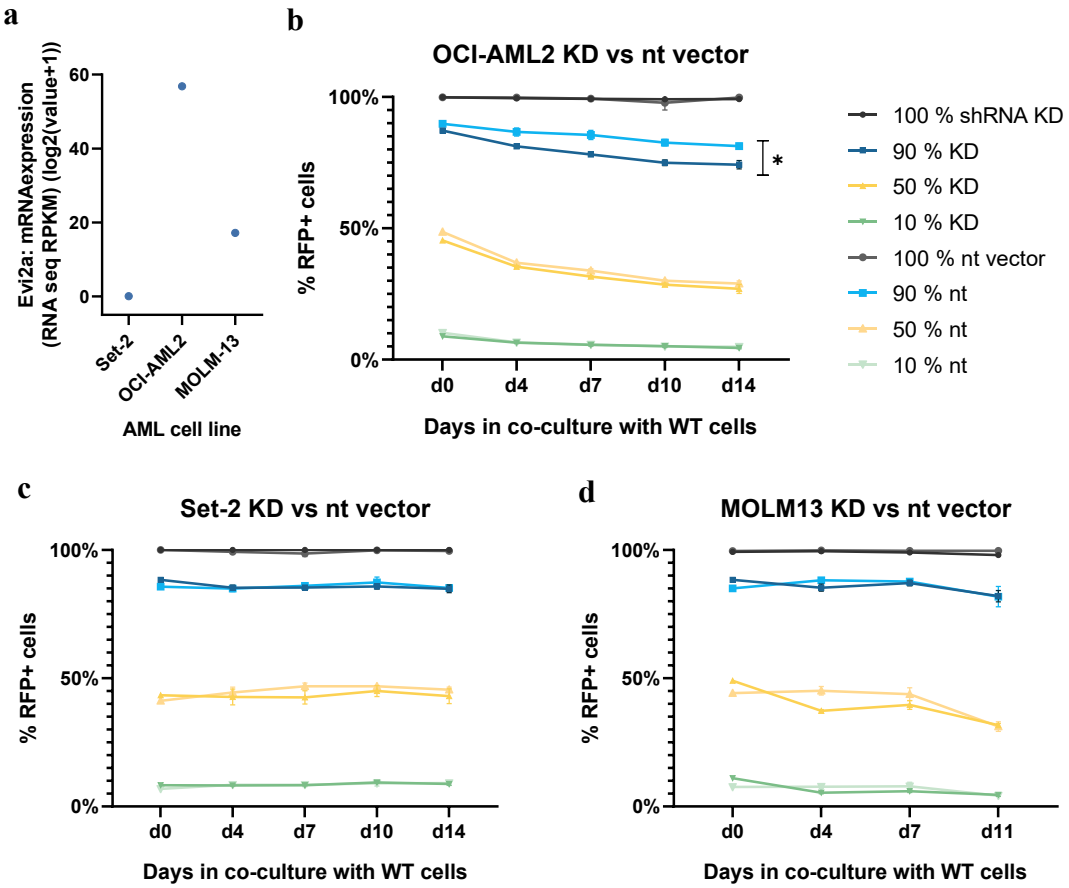

Figure 3: **a)** relative Evi2a expression levels in commonly used human AML cell lines in log2 scale performed by Theo Aurich (according to CCLE Broad 2019), **b-d)** Evi2a KD and non-targeting (nt) competing with WT cells in co-culture experiments in ratios as follows: 100 % KO/nt (black), 90 % KO/wt with 10 % WT (blue), 50 % KO/nt with 50 % WT (yellow) and 10 % KO/nt with 90 % WT, were performed with **b)** MOLM-13 **c)** Set-2 and **d)** OCI-AML2 cells. The percentage of transduced (assessed by RFP expression) was measured on d0, d4, d7 and d11 post co-cultivation.

1.5 Hypothesis and Aim

The driving hypothesis is that Evi2a is essential for adult hematopoiesis and the development of specific subsets of AML. To test the hypothesis functionally, we aimed to:

1.) establish a gene editing platform in AML cell lines and in HSPCs

2.) functionally test the impact of an Evi2a knock-out in AML cells *in vitro* and address the effect in HSPCs *in vivo* by mouse transplantation assays.

2 Materials and Methods

All experiments were planned and performed together with Theo Aurich (supervisor); every step of each experiment was executed by both of us at least once if not stated otherwise. Standard laboratory equipment and consumables was used, purchased from BD, Eppendorf and Gibson. Further, Incubator (Thermo Scientific, HERA cell 150), Laminar hood (Theromo Scientific, SAFE 2020 or HERA safe), Waterbath (Julabo TW20), Microscope (Leica, DMIL), Centrifuge (Centrifuge 5810 R, Eppendorf), Micro Centrifuge (Thermo Scientific, Heraeus Pico 17), Ultracentrifuge (Beckman Couler, Optimal L-90K Ultracentrifuge) Fluorescence-activated cell sorter (FACS) (BD, FACS Aria Fusion II and BD, FACS Aria Fusion), Flow cytometer (BD, LSR Fortessa and BD, LSR II), ScilVet cell counter (Horiba Medical), Biometra TRIO PCR cycler (Analytik Jena), pPCR machine (Applied Biosystems by Thermo Fisher, QuantStudio 5), NanoDrop 1000 (Thermo Fisher), and the mouse facility (Barrier D) were frequently used for experiments and result acquisition. Work was performed in S1 (bench work), BSL2 (cell culture), S2 (Virus production and transduction), mouse facility. Entering the mouse facility, special hygiene and safety measures were followed including protective clothing, a double door system, autoclaved equipment only and handling mice solely in the laminar.

	Reagent	**Brand**	**Lot. Nr.**	**Storage**
Cell culture media	DMEM + GlutaMAX™-I, + 4.5 g/L D-Glucose, + Pyruvate	Gibco	2436444	4 °C
	RPMI-1640 Medium + L-Glutamine + Sodium bicarbonate	Sigma Aldrich	RNBL1764	4 °C
	SpemSpan SFEM, Serum free expansion medium	Stem cell technologies	1000075815	4 °C
Media supplements	P/S	Sigma-Aldrich	0000124656	-20 °C long-term, 4 °C short-term
	L-Glutamine	Thermo Fisher	2342280	-20 °C long-term, 4 °C short-term
	FCS	Gibco	2232584	-20 °C long-term, 4 °C short-term

Other cell culture reagents	DPBS, Dulbecco's Phosphase Buffered Saline	Sigma-Aldrich, Life Science	RNBL1436	RT or 4 °C
	Trypsin – EDTA	Sigma-Aldrich, Life Science	SLCB7231	-20 °C long-term, 4 °C short-term
	Enzyme free dissociation solution	Millipore	10114-1	RT
	Retronectin	Takeda		-20 °C
	Polybrene	Sigma-Aldrich		4 °C
	PEI	Polysciences	23966-1	-20 °C
	pMD2.G (envelope plasmid)	Plasmid Factory	PF1217-200330	-20 °C
	psPAX2 (packaging plasmid)	Plasmid Factory	PF1218-200403	-20 °C
	NaCl	In-house		RT
	Caffein powder	Sigma-Aldrich	BCBQ5381V	RT
	Trypan Blue Solution	Thermo Fisher	BCBZ5425	RT
	Ficoll Paque PREMIUM 1.084	cytiva	10294426	RT
	Dimethyl Sulfoxide (DMSO)	Sigma Aldrich	RNBJ5987	RT
Cytokines	rhFLT3-L (recombinant murine FSM-like tyrosine kinase 3 ligand)	PeproTech	121745	Not lyophilized: -20 °C Lyophilized: -80 °C long term 4 °C short term (2 weeks)
	rmSCF (recombinant murine Stem cell factor)	PeproTech	072178	
	rmTPO (recombinant murine Thrombopoietin)	PeproTech	0121262	
	rhEPO (recombinant murine erythropoietin)	PeproTech	Not available	
	rmIL-3 (recombinant murine Interleukin-3)	PeproTech	011048	
	rmIL-6 (recombinant murine Interleukin-6)	PeproTech	071750	
	rmIL-7 (recombinant murine Interleukin-11)	PeproTech	121951	
	rmIL-11 (recombinant murine Interleukin-11)	PeproTech	0216429	
Bacterial culture	BsmBI-v2	New England Biolabs	76407-370	-20 °C
	2xYT Broth (Capsules)	MP	3012-041-8621	RT
	Carbenicillin	Fisher BioReagents	BP2648-5	-20 °C

	S.O.C. Medium	Invitrogen	1699209	RT
Other	ACK lysis buffer	In house		RT
	Compensation Beads	BD	Not available	4 °C
	Mouse Depletion Dynabeads For untouched Kits	Invitrogen	01139597	4 °C
	Red PCR master mix	Genaxxon	19A2401	-20 °C
	TAE buffer	In house		
	Agarose	Sigma Aldrich	SAP 12656	RT
	Power SYBR Green, PCR Master Mix	Applied Biosystems, Thermo Fisher	2111618	-20 °C
	Ethanol Absolute	Supelco		RT
	ddH2O, UltraPure Distilled Water	Invitrogen		RT
	Antibodies: listed below			

Table 1: List of all reagents used for experiments executed

2.1 Mice

Female C57BL/6 (B6, H-2b) mice were purchased from Janvier-Labs or bred in-house. Experiments were started with the mice of an average age of 6-8 weeks weighing minimum 20 grams. For the competitive transplantation mice with 3 different isoforms of de CD45 surface marker were used. Cells from mice expressing CD45.1 were isolated and used for the knock-out. CD45.1/2 expressing mice were used as competitors and mice harboring CD45.2 isoform were recipients. Up to six mice per cage are kept specific-pathogen-free in individually ventilated filter cages. All animal experiments were performed after acquiring the FELASA permission and in accordance with the Tierschutzgesetz (TierSchG) and Tierschutzversuchstierverordnung (TierSchVersV) in Germany. All experiments were approved by the Animal Care and Use Committees of the German Regierungspräsidium Karlsruhe für Tierschutz und Arzneimittelüberwachung.

2.1.1 Bone Marrow isolation

Mice were sacrificed by cervical dislocation and tibias, femurs, hips, sternum, scapula, and spine were collected in RPMI 1640 on ice. Cells were isolated by crushing the bones and

repeated straining, first through a 100 µm cell strainer and then again through a 40 µm strainer (Greiner bio-one) and topped with RPMI 1640. Cells were then spun down at 1500 rpm for 5 min at RT and resuspended in PBS + 2% FCS (PBS/FCS).

2.1.2 Bone marrow transplantation

Sorted LSK cells (see **2.2.6 Mouse Lin- Sca1+ c-Kit+ (LSK) cells**) were resuspended in PBS/FCS to obtain 20.000 cells in 100 µl. The suspension was mixed with 100 µl supportive BM with a density of 1 x 10^7 cells/ml and immediately transplanted by i.v. tail vain injection into preconditioned CD45.2 recipient mice, that were subjected to TBI (2 x 500 rad). Consequently, a total of 20.000 transduced LSK cells and 100.000 cells supportive BM from CD45.1/2 mice were transplanted into each of the recipients. Two transplantation rounds were performed. In the first cohort, three mice received the Evi2a KO LSK cells, and five mice received the non-targeting (nt) control cells. In the second cohort, in both groups six mice were transplanted. Injecting the mice was solely performed by Theo Aurich.

2.1.3 Blood collection

Blood was obtained by puncturing the vena fascialis, 150 µl of blood were collected into EDTA coated microvette tubes and directly processed or stored on ice for later usage. Bleeding was only performed by me. Blood was lysed by incubating the sample with ACK lysis buffer for 5 min at RT. White blood cells were isolated through centrifugation at 300 x g for 5 min, also at RT. Next the cells were washed with 1.5 ml cold PBS/FCS (centrifugation at 300 x g, 5 min at 4 °C). For staining, the pellet was resuspended in 0.5 ml PBS/FSC containing antibodies for the BTM staining, according to **Table 4**. After 20 min of incubation at 4 °C on the rolling platform, cells were washed with PBS/FCS and resuspended in 0.5 ml PBS/FSC containing DAPI.

2.2 Cell line and primary cell culture

2.2.1 Media compositions

	Reagent	Stock Conc.	Final Conc.
DMEM full medium	DMEM + GlutaMAX™-I, + 4.5 g/L D-Glucose, + Pyruvate	1X	1X
	FCS heat inactivated		10 %
	P/S	50 units Penicillin 50 mg/ml Streptomycin	1 %
RPMI murine full medium	RPMI-1640 Medium + L-Glutamine + Sodium bicarbonate	1X	
	FCS heat inactivated		10 %
	P/S	50 units Penicillin 50 mg/ml Streptomycin	1 %
	rmSCF	100 ng/µl	10 ng/ml
	rmIL-3	100 ng/µl	6 ng/ml
	rmIL-6	100 ng/µl	5 ng/ml
StemSpan full medium	SpemSpan SFEM,		
	P/S	50 units Penicillin 50 mg/ml Streptomycin	1 %
	L-Glutamine	200 mM	2 mM
	rmSCF	100 ng/µl	50 ng/ml
	rmTPO	100 ng/µl	50 ng/ml
	rhFLT3-L	100 ng/µl	50 ng/ml
StemSpan scCFU medium	SpemSpan SFEM,		
	P/S	50 units Penicillin 50 mg/ml Streptomycin	1 %
	L-Glutamine	200 mM	2 mM
	rhFLT3-L	100 ng/µl	10 ng/ml
	rmSCF	100 ng/µl	50 ng/ml
	rmTPO	100 ng/µl	10 ng/ml
	rmIL-3	100 ng/µl	5 ng/ml
	rmIL-11	100 ng/µl	10 ng/ml
	rhEPO	1 IU/µl	0.3 IU/ml
	rmIL-7	100 ng/µl	22.2 ng/ml

Table 2: Media compositions for all perfomed cell culture experiments, DMEM full medium was used for HEK293T and NIH3T3 cells, RPMI murine full medium for MLLAF9 cells, and StemSpan full medium for LSK transduction and LSK scCFU medium for single cell colony forming unit assays in LSK cells.

2.2.2 HEK293T

Human embryonic kidney 293T (HEK293T) cells were cultured in DMEM full medium and split before reaching confluency. Splitting was performed by aspirating medium and washing with PBS, followed by enzymatic detachment using Trypsin – EDTA and incubating for 5 minutes at 37 °C. Detachment was stopped with 2 volumes of DMEM full medium. Desired cell numbers were seeded. Counting was performed using the Cytosmart software (OMNI) or Neubauer chambers. HEK293T cells were used for virus production and titration (**2.4.3 Lentivirus production and titration**).

2.2.3 NIH3T3

NIH3T3 murine fibroblasts were cultured in DMEM full medium and split before reaching confluency. Splitting was performed by aspirating medium and washing with DPBS. Followed by enzymatic detachment using Trypsin – EDTA and incubation for 5 minutes at 37 °C. Detachment was stopped with 2 volumes of DMEM full medium. Desired cell numbers were seeded. The cells were used for the primary validation of the CRISPR/Cas9 system on genomic level. Transduction was performed with a multiplicity of infection (MOI) of 0.3 and 5000 TU/ml. Briefly, 900.000 cells were seeded to T-75 flasks on d0 and on d1 the transduction media (DMEM full medium, 8 µg/ml polybrene, virus) was added onto the cells. Twelve hours after transduction, medium was changed to DMEM full medium. On d3 cells were enzymatically harvested and resuspended in PBS/FCS, stained with DAPI, and sorted for mCherry+ population (at 4 °C).

2.2.4 MLLAF9$^{FLT3(ITD)}$ and MLLAF9^{ctrl}

The murine AML cell lines MLLAF9 cells were donations from Stephen Sykes' lab. Notably, these were transformed from primary LSK cells by introducing MLLAF9 fusion and a FLT3(ITD) mutation in one of the cell lines. Thus, these cells have a slightly more stem-like

phenotype and are therefore dependent on cytokines. If both are addressed in the following, they will be referred to as MLLAF9 cells. Two cell lines were used to confirm that the effect of Evi2a was not specific to the FLT3(ITD) mutation and is evident in different AML subtypes. Both were cultured in suspension in RPMI murine full medium. Cells were kept at 0.2 – 1 x 10^6 cells/ml by refreshing medium regularly. The MLLAF9 cells were used for KO validation on genomic and transcriptomic level, competitive co-culture assays, as well as for optimizing transduction conditions. The cells were transduced with a MOIs ranging from 5 – 25 and 5 x 10^6 TU/ml, MOIs were adjusted for each cell type according to viability, efficiency of transduction and required DNA cutting efficiency. Cells were seeded into T-75 flasks in 2 ml RPMI murine full medium. On the same day, the virus was directly added onto the cells, together with polybrene (8 µg/ml) containing medium. Twelve hours after transduction, the medium was changed by centrifugation at 350 x g, for 5 min at RT and adding fresh RPMI murine full medium. Cells were sorted on d3 after transduction at RT, other than NIH3T3 or LSK cells which are sorted at 4 °C.

2.2.5 MLLAF9^{ctrl} Co-culture assay

Transduced (KO and nt) and WT MLLAF9^{ctrl} cells were co-cultured in ratios of 90:10, 50:50 and 10:90 (also the WT cells were sorted to ensure the same treatment burden) one day after sorting. The percentage of transduced cells was analyzed by flow cytometry every three to four days for two weeks.

2.2.6 Mouse Lin- Sca1+ c-Kit+ (LSK) cells

Lineage Depletion

Whole BM was counted using ScilVet and accordingly diluted to a concentration of max. 3 x 10^7 cells/ml. The first presorting step was performed using “Ficoll-Paque PREMIUM 1.084” (cytiva, 17544602). For this 18.7 ml of Ficoll were pipetted into 50 ml falcon tubes. Next a maximum of 18.7 ml of the diluted cell suspension were carefully layered onto the solution. This is ideally done with a 10 ml serological pipette, to increase the surface area the falcon is tilted. Next the tubes were centrifuged for 30 minutes at 400 x g without a brake at RT. The cells from the interface were then carefully harvested using a 5 ml serological pipette,

as visualized in **Figure 4**. The first harvest was stored on ice. With the remaining liquid and the cell pellet, a second round of Ficoll was performed [14].

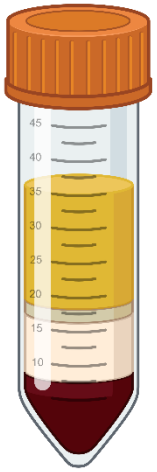

Figure 4: Schematic depiction of Ficoll-based separated blood sample; the interface (beige) containing mononuclear cells was harvested (Created with BioRender.com)

The presorted cells were stained with biotinylated antibodies (Ab) according to **Table 3** (applies for 1 x 10^9 cells). The Ab-cell mix was incubated for 30 min at 4 °C on the rolling platform, followed by washing with ice cold PBS/FCS. Afterwards the pellet was resuspended in PBS/FCS for lineage depletion, while 1 ml per 2 x 10^8 cells was added. Linage depletion was performed using "Mouse Depletion Dynabeads For Untouched Kits" (Invitrogen, by Thermo Fisher Scientific) according to manufacturer's protocol. The beads were washed with PBS/FCS on the magnetic rack prior to usage.

Biotinylated Ab	**Clone**	**Company**	**Volume [µl]**
CD5	2053750	BD Biosciences	250 µl
CD45R (B220)	9352200	BD Biosciences	167 µl
CD11b (Mac-1)	0335767	BD Biosciences	157 µl
CD8a	9092519	BD Biosciences	250 µl
Gr-1 (Ly-6G)	9238330	BD Biosciences	143 µl
Ter119 (Ly-76)	1032072	BD Biosciences	157 µl
Total			**1124 µl**

Table 3: Antibody mix for lineage depletion, volumes for 1 x 10^9 cells

LSK sort and transduction

Next, the cells were counted again using ScilVet for LSK sort staining according to **Table 4**. The cells were initially sorted into StemSpan and then spun down at 500 x g and resuspended in StemSpan full medium. Finally, cells were counted, and 300.000 cells were plated out onto either retronectin-coated plates [15] or ultra-low attachment plates and cultivated for transduction. The cultivation duration was minimized to avoid *in vitro* differentiation. Retronectin coating was performed according to the manufacturer's protocol yielding 7 µg/cm^2. Six to twelve hours after cultivation, the cells were transduced. Briefly, medium was gently aspirated ´by pipetting. Next, half of SpemSpan full medium, containing 4 µg/ml polybrene, was added to the cells, followed by adding the virus, and then the other half of the media, to provide equal spreading of the virus. Again, twelve hours later, the medium change was performed by carefully aspirating the medium using a pipette and gently adding fresh media. Another 36 h later, the cells were harvested using an enzyme-free detachment buffer. Briefly, the supernatant was transferred into a tube. Next the wells are washed with PBS/FCS, and the wash was transferred to the same tube. For gentle detachment, enzyme-free detachment buffer was added and incubated for 5 min at 37 °C. Detached cells were added into the same tube again and wells were washed with PBS/FCS, followed by transferring it into the same tube, until no more cells are evident in the wells. Cells were centrifuged (500 x g, 5 min, 4 °C) and stained with DAPI. The top 30 % mCherry expressing cells were sorted and subsequently transplanted to create the Evi2a KO mouse model. Transduction of LSK cells was performed using an MOI of 25 and 5 x 10^6 TU/ml. MOIs were chosen in accordance to the cell vulnerabilities and adjusted throughout the experimental process.

2.2.7 Single Cell Colony Forming Unit Assay (scCFU)

LSK cells were sorted into two 96-well plates with StemSpan full expansion medium (**Table 2**) for each, KO, nt and wild-type (WT) cells. After ten days of incubation, the colonies in each plate were counted, and in addition, DNA of ten colonies was isolated and sent for sanger sequencing.

2.3 Flow cytometry and fluorescent activated cell sorting (FACS)

2.3.1 Flow cytometry analysis

Relative number of transduced cells

For titration, checking transduction efficiencies and dynamics in co-culture assays, cells were only stained with DAPI directly prior to data acquisition. The gating strategy is depicted in **Figure 5a**. Briefly, to assess the relative number of transduced cells the gates were set to mCherry on the y axis and FCS-A on the x axis, or via a histogram. The mCherry+ population represents the successfully transduced cells (as exemplified in the bottom graphs of **Figure 5a**). Analysis was performed on BD LSR Fortessa or BD LSR II.

Check supportive bone marrow

BM from C57BL/6 CD45.1/2 mice was isolated according to 2.1.1 **Bone marrow isolation**. A 200 µl aliquot was stained with 1:300 anti-CD45.1 conjugated to PE-Cy7 (A20, Invitrogen) and 1:100 anti-CD45.2 conjugated APC (104, Invitrogen) for 20 min at 4 °C on the rolling platform. Cells were washed with PBS/FCS and resuspended in 200 µl PBS/FCS + 1 µg/ml DAPI. Gates were set to CD45.1 against CD45.2 (**Figure 5b**). If cells are double positive, the BM is feasible for transplantation. Supportive BM chimerism was checked prior sorting with BD FACS Aria Fusion II or BD FACS Aria Fusion.

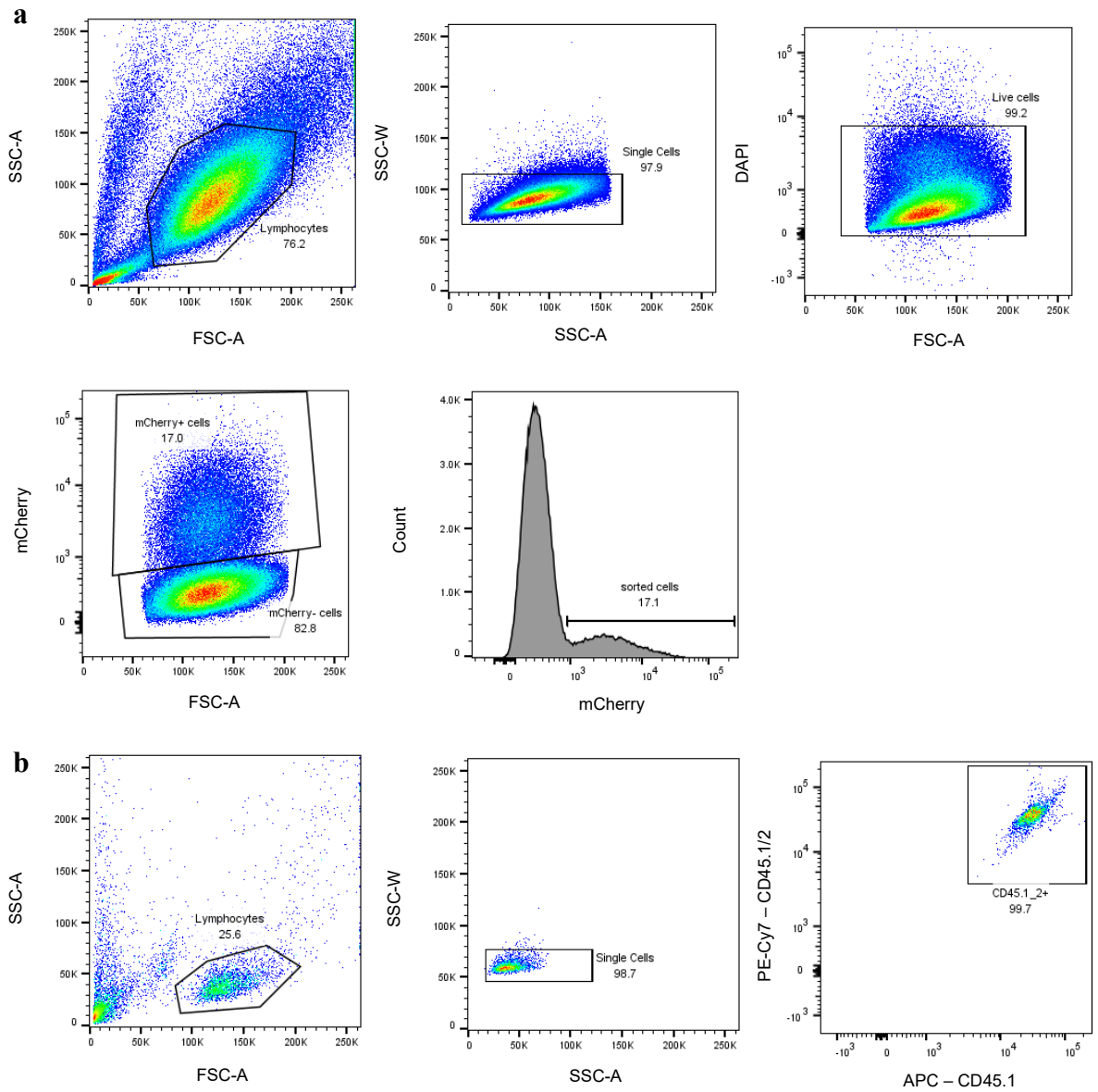

Figure 5: Gating strategy for a) successfully transduced cells by gating for mCherry+ population and **b)** validating CD45.1/2 in supportive BM CD45.1 in PE-Cy7 (YG-780/60), CD45.2 in APC (RL-670/14)

2.3.2 LSK sorting

Lineage depleted cells were stained according to **Table 4**, using 1 ml Ab mix for 1 x 10^8 cells. The stained cells were incubated for 20 min at 4 °C on the rolling platform. Cells were washed, resuspended in PBS/FCS and stained with DAPI just before sorting.

First, cells, singlets and live cells were determined. Next, to exclude Lineage+ cells, gates were set for Sca-1 (APC-Cy7) and Streptavidin (PE). To get the LSK cells, cKit (APC) was plotted against Sca-1- and double positive cells were sorted. The exact gating strategy is plotted in **Figure 6**. Cells were sorted into 15 ml falcons with BD FACS Aria Fusion II or BD FACS Aria Fusion under sterile conditions. Sorting was only done under supervision of Theo Aurich.

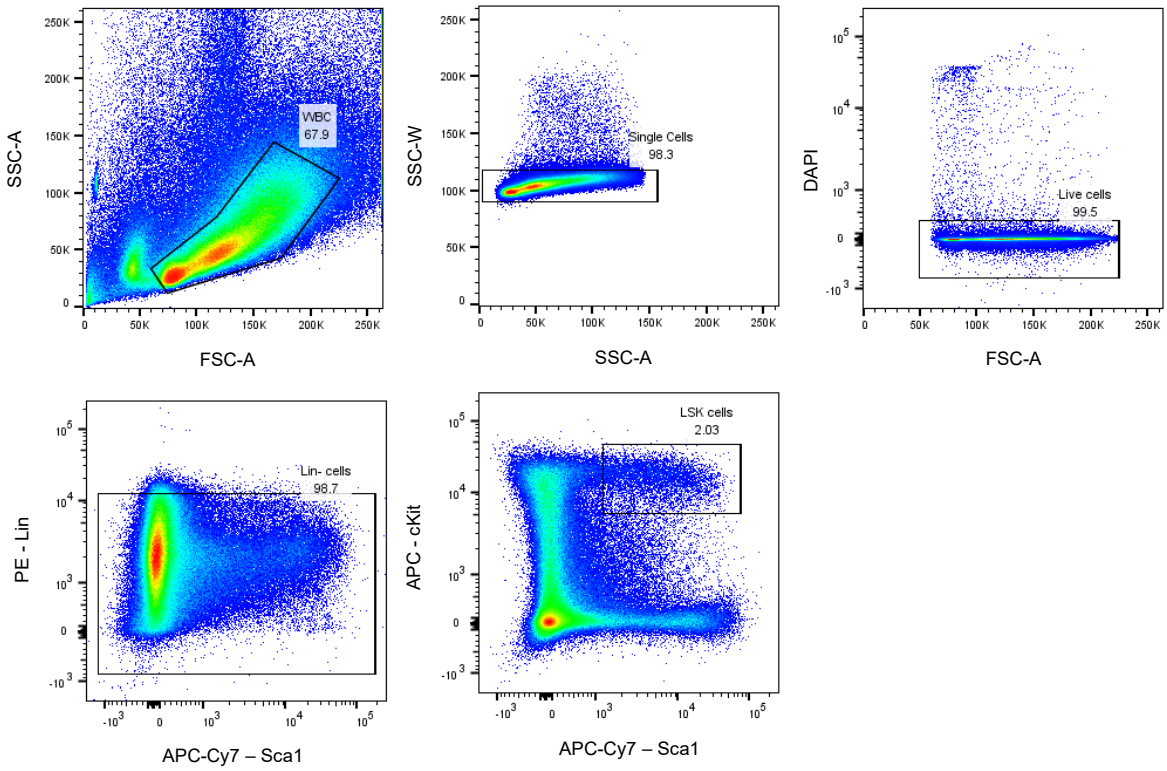

Figure 6: Gating strategy for LSK cell sort using the following staining: Lin- (PE) Sca1+ (APC-Cy7) cKit+ (APC)

2.3.3 Peripheral blood analysis

For checking the major blood parameters *in vivo*, B cell-, T cell-, myeloid- (BTM) staining was used; see **Table 4**.

The diluted Abs were added to the cell suspension and incubated at 4 °C for 20 min, followed by a washing step. Shortly before the measurement, DAPI was added. The cells were analyzed and sorted on BD FACS Aria Fusion II or BD FACS Aria Fusion. DNA of the sorted cells was then isolated, 1) PCR amplified and sent for sanger sequencing and 2) used for qPCR to assess

the frequency of cells carrying Cas9. Gating for the BTM sort, donor chimerism analysis are plotted in **Figure 7**. Sorting of the cells was only done under supervision of Theo Aurich.

	Antibody	**Fluorophore**	**Clone**	**Company**	**Dilution**
LSK sort	Streptavidin	PE	-	Invitrogen	1:100
	CD117 (c-Kit)	APC	2B8	Invitrogen	1:2000
	Sca-1	APC-Cy7	D7	BD Pharmigen	1:1000
	DAPI	DAPI	-	Thermo Scientific	1:1000
Supp BM	CD45.1	PE-Cy7	A20	Invitrogen	1:300
	CD45.2	APC	104	Invitrogen	1:100
BTM sort and analysis	CD4	PE-Cy7	GK1.5	Invitrogen	1:1000
	CD8	PE-Cy7	53-6.7	Invitrogen	1:1000
	B220	PE-Cy7	RA3-6B2	Invitrogen	1:1000
	B220	APC-Cy7	RA3-6B2	Invitrogen	1:300
	Gr1	APC-Cy7	RB6-8C5	Invitrogen	1:2000
	CD11b (Mac-1)	APC-Cy7	M1/70	Invitrogen	1:1000
	CD45.1	BUV395	A20	BD Horizon	1:300
	CD45.2	APC	104	Invitrogen	1:100
	DAPI	DAPI	-	Thermo Scientific	1:1000

Table 4: LSK sort: Abs for LSK sort, streptavidin binds biotin on Lin+ cells (see lineage depletion), LSK marker (c-Kit and Sca-1) and DAPI for live cells; **Supp BM**: to validate CD45.1 and CD45.2 expression in supportive bone marrow from competitor; **BTM** (B cell, T cell, myeloid cells) **sort and analysis**: Ab staining panel for donor (CD45.2) derived: T cells (CD4, CD8), B cells (B220), myeloid cells (Gr1, CD11b), including staining for donor (CD45.1), supportive bone marrow (CD45.1 and CD45.2), and recipient (CD45.2) and DAPI for live cells

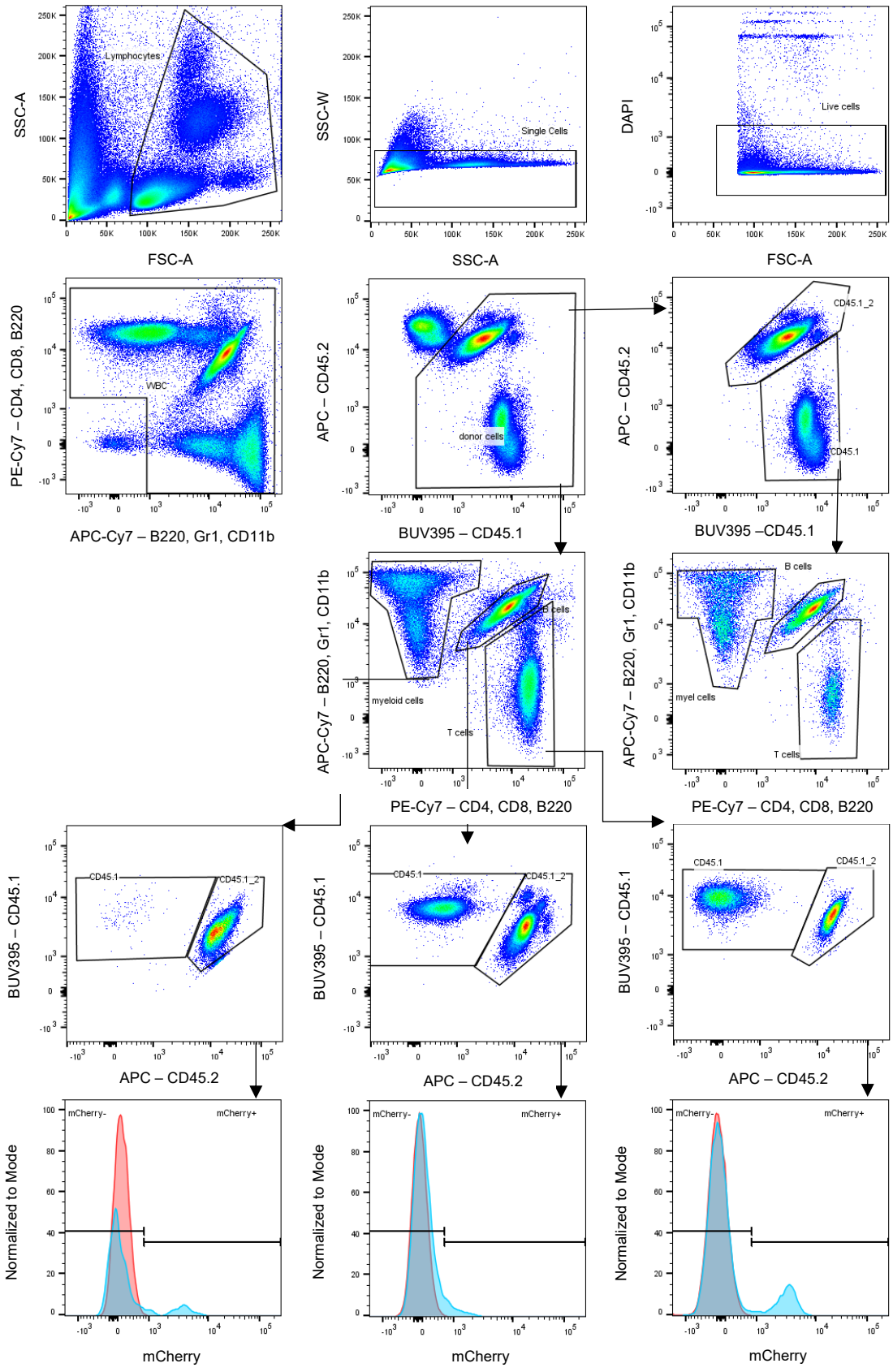
SSC-A
FSC-A
Lymphocytes
SSC-W
SSC-A
Single Cells
DAPI
FSC-A
Live cells
PE-Cy7 – CD4, CD8, B220
APC-Cy7 – B220, Gr1, CD11b
WBC
APC – CD45.2
BUV395 – CD45.1
donor cells
CD45.1_2
CD45.1
APC – CD45.2
BUV395 –CD45.1
APC-Cy7 – B220, Gr1, CD11b
PE-Cy7 – CD4, CD8, B220
B cells
myeloid cells
T cells
myel cells
BUV395 – CD45.1
APC – CD45.2
Normalized to Mode
mCherry
mCherry-
mCherry+

Figure 7: Gating strategy for PB blood analysis, gating for WBC to total donor cells and next to CD45.1 donor or BTM followed by donor chimerism including mCherry expression.

2.4 CRISPR/Cas9 design

2.4.1 Vector design

The lentiCRISPRv2-mCherry construct was used since primary cells should be transduced. Initially four guide RNAs (gRNA), 1 (5'- AAACCGTCGTCTTCTGGAACAAGAC-3'), 2 (5'-AAACTGGGTCACAAGGTGAGCGCC-3'), 3 (5'-AAACCCTGACTTTTGATCTCTGCTC-3') and 4 (5'-AAACTATCTGTACCTTTCTATTTC-3') targeting *evi2a* were designed using "CRISPick" software (https://portals.broadinstitute.org/gppx/crispick/public) and tested for KO efficiencies. An additional nt gRNA was used as a control; both, the pLentiCRISPRv2-mCherry vector and a ready to use nt vector were gifted from Rene Jackstadt. Transcription of the guides is controlled by a U6 promotor. The entire construct of the vector is shown in **Figure 8** [1]. Cloning of the gRNAs into the vector was performed according to the protocol provided by *Zhang et al.* (2013) [4], [16], [17]. Briefly, first the CRISPR plasmid was digested and dephosphorylated using BsmBI-v2 for 15 min at 55 °C. Second, an agarose gel was run with the product and the larger band (the vector backbone) was purified using "QIAquick Gel Extraction Kit" (Qiagen, Cat. No. 28706). Next each pair of oligos was phosphorylated and annealed in the thermocycler (37 °C for 30 min, 95 °C for 5 min, ramp down to 25 °C at 5 °C/min) followed by ligation. The vector was then transformed into One Shot™ Stbl3™ E. coli.

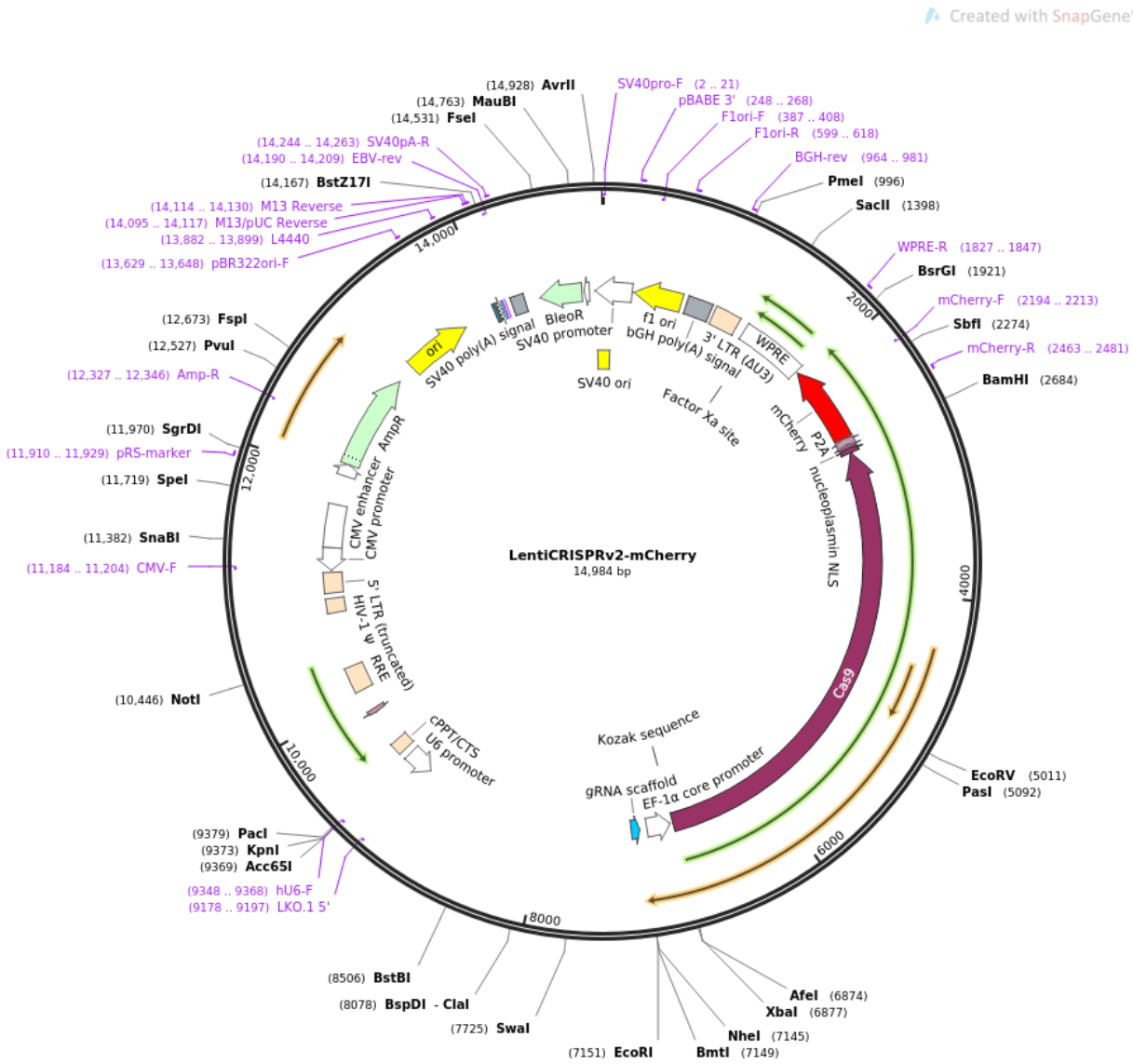

Figure 8: LentiCRISPRv2-mCherry was a gift from Agata Smogorzewska (Addgene plasmid #99154; http://n2t.net/addgene:99154 ; RRID:Addgene_99154), provided by Rene Jackstadt [18]

2.4.2 Plasmid production

Vectors for each guide described above were transformed in One Shot™ Stbl3™ chemically competent cells. Briefly, 5 µl of DNA were added to each vial and incubated on ice for 30 min. Next the cells were heat shocked for 45 sec at 42 °C and moved back to ice for 2 min. To each vial, 250 µl of prewarmed S.O.C. medium was added and incubated horizontally for one hour at 37 °C in the shaking incubator at 300 rpm. Finally, 25 µl from each transformation was

spread onto prewarmed selective plates (2YT agar with 50 µg/ml carbenicillin) and further incubated overnight. Single colonies were picked from each transformation reaction, transferred into 2YT medium containing 50 µg/ml carbenicillin and further incubated at 32 °C [19] in the shaking incubator until the media turned turbid indicating bacterial growth. Finally, the plasmids were collected using "QIAprep Spin Miniprep Kit" (Qiagen, Cat. No. 27106) and sent to eurofins genomics for sanger sequencing (https://eurofinsgenomics.eu). The clones with the highest sequencing qualities were used for the "QIAGEN Plasmid Maxi Kit" (Qiagen, Cat. No. 12163) for large scale plasmid acquisition.

2.4.3 Lentivirus production and titration

The virus was produced using HEK293T cells, which were initially seeded into DMEM full medium to reach 70 % confluency (2 x 10^6 cells per T-175 flask) on d0. On d1 day, cells were transfected by applying a three-plasmid transfection system, with a 1:1:1 molar ratio of the envelope plasmid (pMD2.G), the packaging plasmid (psPAX2) and the transfer plasmid (1, 2, nt), and 5.5 µg PEI (1 µg/µl) per 1 µg DNA. A total plasmid concentration of 1.05 µg/ml was achieved. Per flask, 2 ml of the transfection mix was added to the cells in 18 ml DMEM full medium. Between 12 – 24 h post transfection the medium was changed to DMEM full medium, containing 4 mM concentrated Caffein, while keeping 3 ml of the old medium. Another 48 h post transduction, the virus was harvested by ultracentrifugation (25.000 rpm, 2 h, 4 °C), resuspended in PBS or StemSpan and stored at -80 °C.

To determine the virus concentration, 50.000 HEK293T cells were seeded to a 24-well plate on d0. Just before transduction, 3 control wells were counted and the average was calculated. The virus was added in serial dilutions of 1:10 – a schematic of dilution is shown in **Figure 9**. The medium was changed on d2; another two days later, the transduction efficiency was evaluated using flow cytometry by measuring the mCherry+ population. The titer in transducing units per ml [TU/ml] was determined according to 1: Viral titer calculation.

.

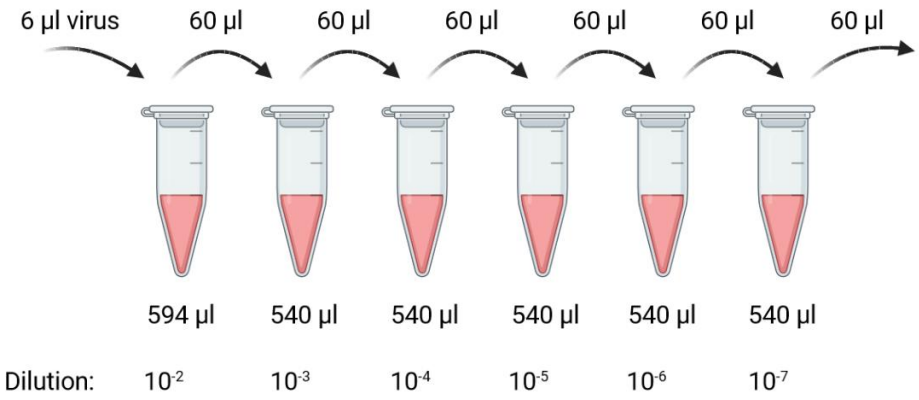

Figure 9: Schematic depiction of serial dilution for lentivirus titration (Created with BioRender.com)

1: Viral titer calculation

$$Viral\ Titer\ = \frac{transducing\ units\ (TU)}{ml} = \frac{number\ transdcued\ cells\ \times percent\ fluorescent}{virus\ volume\ in\ ml}$$

Several rounds of virus production followed by titration were performed, yielding titers between 1 x 10^6 to 1 x 10^9. Transductions of MLLAF9 and LSK were only performed with titers > 1 x 10^8 to reduce the amount of viral supernatant added to the cells. The virus batches with the according titers and experiments they were used for are shown in **Table 5**.

Virus batch ID	gRNA	Titer [TU/ml]	Experiments
Virus batch 1 (VB1)	1	2.21×10^7	KO validation in NIH3T3
	2	7.39×10^7	
	3	2.63×10^7	
	4	6.92×10^7	
	nt	1.15×10^7	
Virus batch 2 (VB2)	1	5.81×10^6	KO validation in NIH3T3, MLLAF9 and LSK cells
	2	5.58×10^6	
	nt	6.89×10^6	
Virus batch 3 (VB3)	1	1.26×10^9	KO validation in MLLAF9 and LSK cells
	2	7.26×10^9	
	nt	7.41×10^8	
Virus batch 4 (VB4)	1	5.22×10^7	KO validation in MLLAF9 and LSK cells
	2	1.59×10^8	
	nt	2.32×10^8	
Virus batch 5 (VB5)	1	4.17×10^8	LSK transplantation
	2	2.86×10^8	
	nt	1.72×10^8	
Virus batch 6 (VB6)	2	1.95×10^9	KO validation in MLLAF9 and LSK transplantation
	nt	1.16×10^9	

Table 5: Virus batches produced, including the measured titers and corresponding experiments.

2.5 PCR and sanger sequencing

Before sending in samples for sequencing, DNA was PCR amplified. PCRs against *evi2a* were performed using "Genaxxon Red MasterMix (2x)" (Genaxxon, Bioscience) using the forward primer (5'-GGAAAGGACAAACGCACTTC-3') and reverse primer (5'-CATTGGGAATTTGACATCTGC-3') in 10 µM concentrations. Cycling conditions were set as following: initial denaturation of 3 min at 95 °C, followed by 35 cycles of denaturation for 30 sec at 95 °C, annealing for 30 sec at 60 °C and extension for 1 min at 72 °C and final extension for 10 min at 72 °C. The product was either, directly purified using "QIAquick PCR Purification Kit" (Qiagen, Cat. No. 28106) or run on a 1.5 % agarose gel for 40 min at 130 V and subsequently purified using "QIAquick Gel Extraction Kit" (Qiagen, Cat. No. 28706). In

both cases, the product was eluted in RNase free ddH_2O. The purified PCR product was sent for sanger sequencing to eurofins genomics, using supreme run tube or light run tube. The sequencing results were analyzed by tracking of indels by decomposition (TIDE) program (TIDE (nki.nl).

2.6 qPCR

2.6.1 Quantitative PCR

The genomic DNA was diluted in ddH_2O to yield 10 ng/µl. For the qPCR, "PowerSYBR Green PCR Master Mix" (Applied Biosystems, by Thermo Fisher Scientific) was applied, using the primers according to Table 6. The reactions were filled up with ddH2O to 12.5 µl per reaction. For each gene and target, three replicates were made. The reactions were run in a 356-qPCR plate on QuantStudio5 qPCR machine, applying the $2^{-\Delta\Delta Ct}$ qPCR method (Applied Biosystems, by Thermo Fisher Scientific) and analyzed using "QuantStudio Design & Analysis Software v1.4.3". Relative quantification of the target (Cas9) against the reference gene (ApoB) was calculated according to 2: Relative Quantification Calculation. With Time 0 representing 1x target expression and Time x referring to any time point [20]. Pipetting of all qPCRs was performed by myself.

2: Relative Quantification Calculation

$$\Delta\Delta C_T = (C_{T,Target} - C_{T,Reference})_{Time\ x} - (C_{T,Target} - C_{T,Reference})_{Time\ 0}$$

Primer		**Sequence**	**Reaction volume from 10 µM stock [µl]**	
Cas9 [21]	*fwd*	5'-GGACTCCCGGATGAACACTA	0.125	qPCR
	rev	5'-TCGCTTTCCAGCTTAGGGTA	0.125	
ApoB [22]	*fwd*	5'-CACGTGGGCTCCAGCATT	0.125	
	rev	5'-TCACCAGTCATTTCTGCCTTTG	0.125	

Table 6: primer and concentrations used for RT-qPCR and qPCR

2.7 Statistics

Statistical analyses were performed in “GraphPad PRSIM 9.2.0” software. Each experiment was performed with a minimum biological replicate number of n = 3. Statistical comparisons were calculated using student’s two-tailed *t*-test to assess significance; p values < 0.05 were chosen as cutoff. For comparison of multiple independent groups one-way ANOVA was performed. Significant results are marked accordingly. The bar graphs depict mean ± SEM.

3 Results

3.1 Production of the lentiviral CRISPR/Cas9 system carrying the gRNAs was successful

To investigate the functional role of Evi2a, we generated a loss-of-function via CRISPR/Cas9 mediated gene disruption. The 4 gRNAs were cloned into previously digested vector. The backbone was isolated from the gel and afterwards sent for sanger sequencing. The correct insertion of the gRNA was confirmed by aligning the sequences (SnapGene). All analyzed plasmids aligned to the reference plasmid and the guides were not altered. For large scale transfection, the following clones were expanded (based on best alignment to the reference): guide 1: clone #1, guide 2: clone #2, guide 3: clone #3 and guide 4: clone #1. The DNA content of all plasmids was measured using the Nanodrop 1000 and are shown **Table 7**.

Plasmid	Concentration
guide 1	1188 ng/µl
guide 2	1129 ng/µl
guide 3	1070 ng/µl
guide 4	1609 ng/µl
Non-targeting guide	1044 ng/µl

Table 7: measured DNA yield in ng/µl of plasmids carrying gRNAs against Evi2a measured using "NanoDrop 1000"

3.2 Genetic lesions were introduced in all tested cells

3.2.1 CRISPR/Cas9 gRNA delivery is effective and stable in NIH3T3 cells

Initially a pilot experiment with all guides (virus batch 1) was performed to select for the best gRNA in NIH3T3 cells. Guide 1 and guide 2 showed higher DNA cutting efficiency compared to guide 3 and 4 (data not shown). Therefore, for sorting and downstream analysis, murine fibroblasts were infected with both guide 1 and guide 2 (virus batch 1) and an MOI of 0.3. Of note, the MOI was not adjusted further because the experiment was solely used to validate the

correct cutting location of the vector. The transduction efficiency was measured in FACS sorted mCherry+ cells 7 days post transduction. For the lentivector carrying the nt sgRNA (hereafter as nt control), KO guide 1 and guide 2, 17.2 %, 31.1 % and 6.5 % mCherry+ cells were yielded respectively (**Figure 11a**). To assess whether the introduction of the virus induced disruption of the target gene locus, DNA of mCherry expressing cells was subjected to sanger sequencing. Sequencing was done either directly or after 7 and 13 days in culture. Notably, by day 7 cultured cells maintained mCherry+ expression at around 90 %, while by day 13 the expression increased to nearly 100 % (assessed by flow cytometry, **Figure 11b and c**). The percentage of WT DNA sequenced decreased with time in culture, reaching a plateau after about 14 days. this data indicated that Cas9 integrated even one to two weeks after initial transduction (**Figure 11d**). Presumably in the initially sorted cells not all alleles were gene manipulated, while after two weeks the majority of alleles were disrupted at the Evi2a locus. Cutting efficiencies proved to be higher in the guide 2. Therefore, following experiments were largely performed using guide 2.

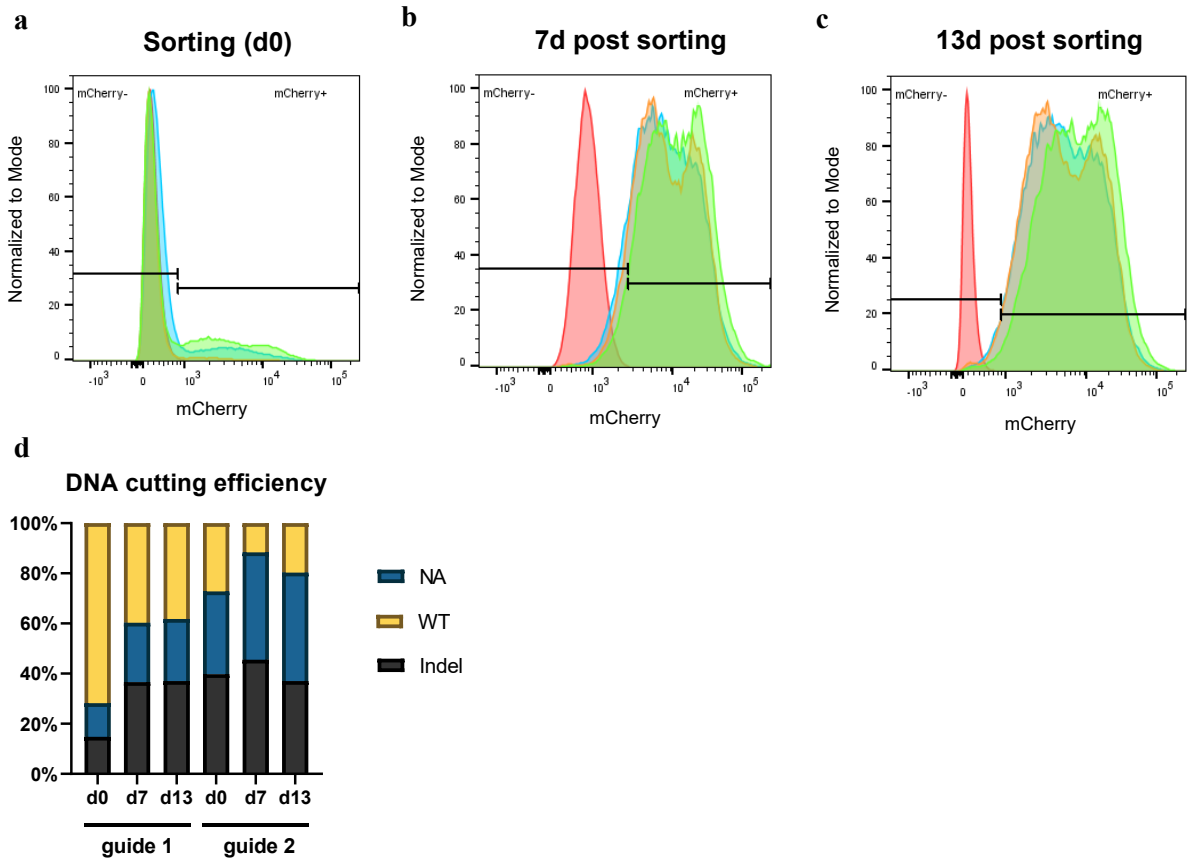

Figure 10: NIH3T3 mCherry expression of guide 1 (green), guide 2 (orange) and nt vector (blue) compared to non-transduced cells (red) a) at the sort on day 7 **b)** on day 7 after the sort **c)** on day 13 after the sort **d)** genomic cutting efficinecy assessed by sanger sequencing and TIDE analysis at day of sort (d0), 7 days after soring (d7) and 13 days after soring (d13) (NA = out of measurable range)

3.2.2 KO introduction in MLLAF9$^{FLT3(ITD)}$ and MLLAF9^{ctrl} cells is less effective and no *in vitro* functional effect is evident

For assessing the transduction and cutting efficiency, and assessing the KO on the transcriptional level, the same procedure was performed in murine myeloid cell lines. Two different lines were used (one bearing an additional FLT3(ITD) mutation), to rule out effect of the presence or absence this mutation on the Evi2a KO.

To find the most optimal transduction conditions, different transduction periods, MOIs and higher and lower virus concentrations, i.e., TU/ml (for nt: 2 x 10^6 and 4 x 10^6, for KO guide: 3 x 10^6 and 1 x 10^7) were tested (using VB3 and VB4). In addition, the influence of adding

polybrene, a transduction enhancer [23], was assessed. In **Figure 11a**, the conditions tested are visualized. Longer incubation with the virus proves to increase the percentage of mCherry+ cells. Furthermore, the MOI had less influence on the efficiency than the concentration of the virus in the transduction media. Besides relative transduction efficiency, also cell death was considered since we were aiming for a high absolute number of KO cells. Taking both efficiency and viability into consideration, 12 h transduction, a MOI of 25 and 5 x 10^6 TU/ml proved to be most successful (visualized in **Figure 11a,** very right bar).

In **Figure 11b** the percentage of transduced cells on d3 after the transduction is visualized, aiming at 45 % to 80 % transduction efficiencies when using VB2. In another experimental setup, VB6 was used for transduction; however only about 20 % of the cells are successfully transduced on d2 (**Figure 11c**). To assess the temporal effects in transduction, another set of cells was infected with 2 virus batches (VB3 and VB6) and sorted on d3. In accordance with the previously observed delay in Cas9 insertion, transduction efficiencies in the cells infected with VB6 increases to 33 % (**Figure 11d**). The other tested batch has even higher efficiencies of 54 % (**Figure 11e**), showing variance between different batches, even though comparable titers were measured. In accordance with NIH3T3 cells, the relative amount of uncut DNA steadily decreases with time, visualized in **Figure 11f**, although the cutting efficiency already proved to be high at day 7. To functionally assess the effect of Evi2a, an *in vitro* competitive co-culture assay was set up (only using MLLAF9^{ctrl} for simplicity). For that, WT cells were cultured in different ratios together with either KO cells, or cells transduced with the nt vector. The percentage of cells expressing mCherry was assessed by flow cytometry on d0, d4, d7, d11 and d14 after seeding. The percentage KO cells were then compared to the nt cells to assess whether the deletion of Evi2a affects competitive growth towards WT cells. The experiment shows that the KO in MLLAF9^{ctrl} cells does not impair proliferation, as shown in **Figure 11g**. The cells transduced with the nt vector, and the KO cells have the same growth disadvantage as opposed to WT cells. Since a decrease in mCherry expressing cells is detected, even if 100 % transduced cells are seeded, probably some WT that fell into the sorting gate having a growth advantage. The impaired growth of the nt cells is most likely due to the stress and toxicity the cells are exposed to during lentiviral transduction. Since AML cell lines were used, this data also suggests that Evi2a is not essential for AML persistence.

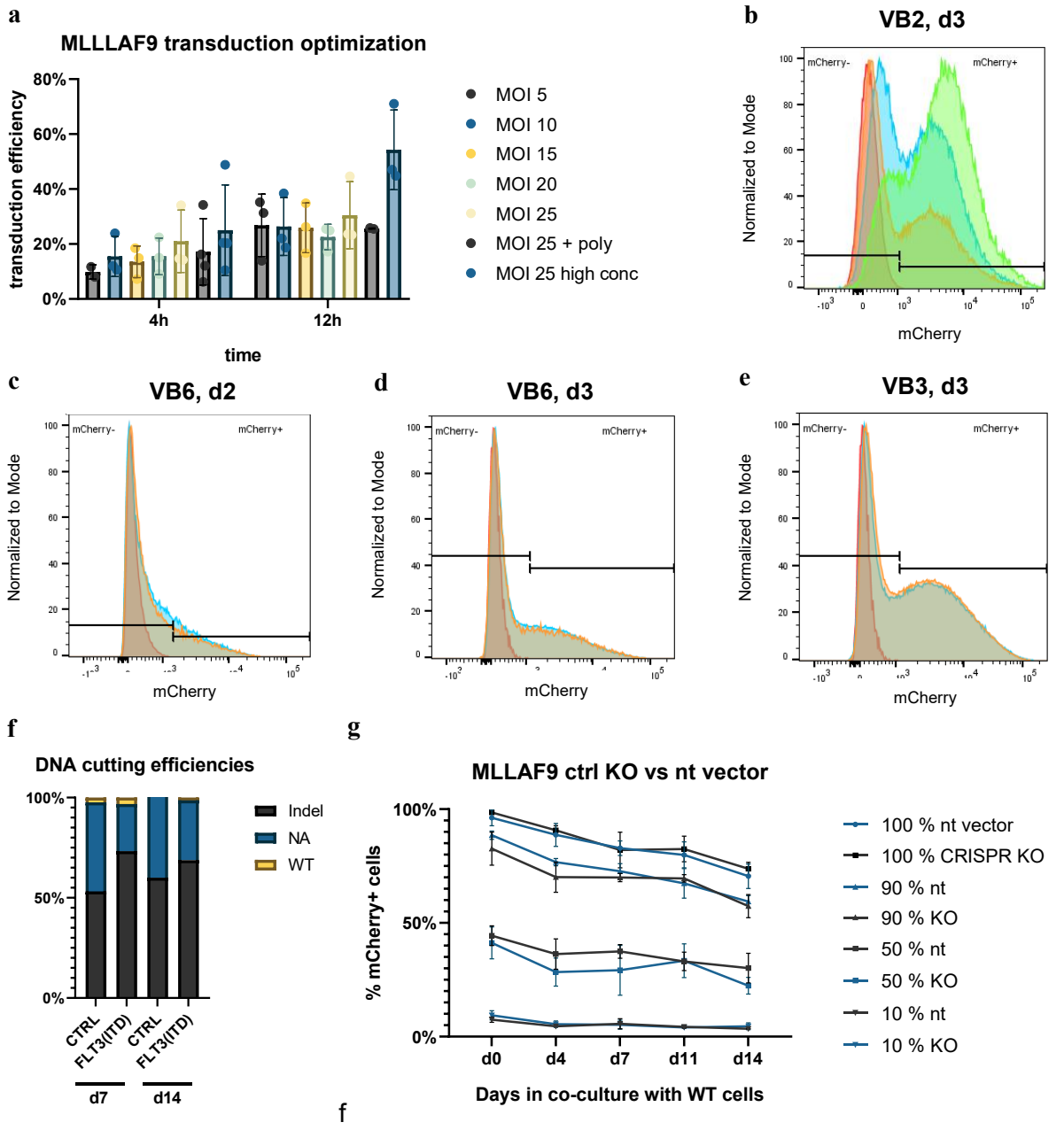

Figure 11: a) optimization of transduction conditions using multiplicities of infection (MOI) ranging from 5 to 35 and TU/ml of 2 x 10^6 and 4 x 10^6 (high) for nt, 3 x 10^6 and 1 x 10^7 (high) for guide 2, data was pooled **b-e)** MLLAF9 transduction efficiencies of guide 1 (green), guide 2 (orange) and nt vector (blue) compared to non-transduced cells (red) in **b)** FLTT(ITD) cells using VB2, 3 days **c)** ctrl cells using VB6, 2 days **d)** ctrl cells using VB6, 3 days **e)** ctrl cells using VB3, 3 days **f)** genomic disruption of Evi2a locus 7 days and 14 days after sorting mCherry+ population, in $MLLAF9^{FLT3(ITD)}$ and $MLLAF9^{ctrl}$ assessed by sanger sequencing and TIDE analysis (NA = out of measurable range) **g)** competitive co-culture of WT and mCherry+ transduced cells in seeding ratios of 90:10, 50:50 and 10:90, percent nt cells (blue) are plotted in comparison to KO cells (black)

3.2.3 mCherry expression is less pronounced in transduced LSK cells

In the next step, the transduction was tested in primary stem and progenitor cells, before transplantation. Given the low mCherry signal observed in LSK cells, we firstly optimized the transduction and sorting protocol. To reevaluate the ideal transduction conditions, MOIs ranging from 25 to 100 and TU/ml of 5 x 10^6 to 2 x 10^7 were applied. The absolute cell number sorted in the different conditions are visualized in **Figure 12b**. When transducing with a high number of infecting particles (2 x 10^7) the transduction efficiency is lowest, probably caused by viral toxicity or a lack of nutrients due to a low media volume. The other three conditions resulted in similar absolute counts of about 350.000 KO cells. Considering technical applicability of the system (i.e., providing enough media to avoid starvation and reduce the amount of virus consumption), further transductions were performed with a MOI of 25 and 6 x 10^6 TU/ml. The outlier in the chosen condition may be considered as a technical error. When plotting the mCherry histograms against each other, a general yet slight shift of the mCherry peak of transduced cells compared to WT cells was evident (**Figure 12a**). Notably, a higher mean fluorescent intensity (MFI) was seen in the cells transduced with the nt vector (blue). The reason for the general shift in MFI instead of a distinct mCherry+ population remains unclear. Regardless, several sorting attempts were made, to find the ideal gating to achieve high genetic disruption whilst not losing potentially transduced cells. Finally, sorting the highest 30 % of the mCherry gate proved to achieve satisfying results according to sanger sequencing (data not shown). To additionally validate the knock-out at the Evi2a locus in the cells that will be transplanted, cells were cultured for ten days and sent for sanger sequencing. As shown in **Figure 12c** approximately 5 % of the transplanted LSK cells remained WT. The high degree of cut DNA was attributed to the prolonged time in culture, that was previously observed in cell lines. The data indicated that the degree of mCherry intensity cannot be directly translated to the KO efficiency, data on the effect of lentiviral transduction using a chosen vector in LSK cells will help unravel the for us to date unclear dynamics.

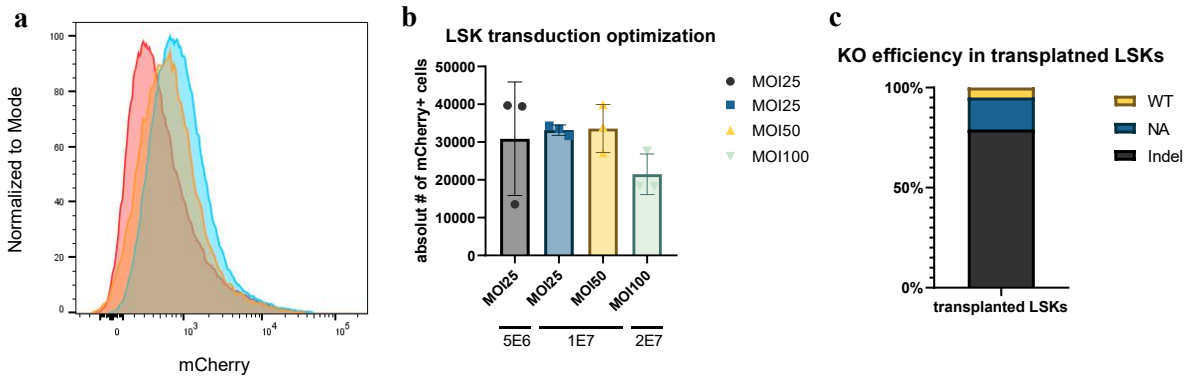

Figure 12: a) LSK transduction efficiencies of guide 2 (orange) and non-targeting vector (blue) compared to non-transduced cells (red) **b)** transduction optimization using MOIs ranging from 25 to 100, and TU/ml ranging from 5 x 10^6 to 2 x 10^7 **c)** KO efficiency of transplanted cells (first cohort) assessed by sanger sequencing and TIDE analysis (NA = out of measurable range)

3.3 Transplanted KO LSK cohorts expanded to different degrees during *in vitro* transduction

Having established a successful Evi2a KO *in vitro*, we wanted to interrogate the role in the *in vivo* setting. For that, a competitive transplant was set up, in which each recipient mouse is transplanted with 20.000 mCherry+ CD45.1 donor cells, and 150.000 CD45.1/2 supportive bone marrow cells. Two cohorts were set up, in the first approach approximately 2 x 10^6 LSK cells were sorted for transduction. When resorting the top 30 % mCherry expressing cells, only 119.000 cell of the nt group and 75.000 cells of the KO could be sorted and transplanted into five and three recipients respectively, each receiving 20.000 cells. The difference in the cell counts is most likely attributed to varying toxicity of the individual viral supernatants. In the second cohort only 6 x 10^5 LSK cells could be acquired for transduction. When resorting the top 30 % mCherry+ population we got 140.000 cells in both groups and transplanted six recipients for each.

3.3.1 Donor chimerism is not altered in the KO compared to the nt control because WT CD54.1+ LSK cells expand

To assess the reconstitution potential of the transplanted KO cells, peripheral blood was analyzed four weeks, eight weeks, and twelve weeks (only the first cohort) post transplantation. The donor chimerism, i.e., the percentage of transplanted mCherry+ LSK cells (CD45.1) opposed to the CD45.1/2 supportive BM cells, was assessed via flow cytometry. In addition, the relative numbers of donor B, T, and myeloid cells were analyzed. This is done by first gating for CD45.1+ population, followed by the BTM gating (visualized in **Figure 7**). The respective mCherry expression for all populations was measured, by gating for any cell type and then plotting a histogram with mCherry using the WT as a gating reference. Moreover, the KO in the peripheral blood cells was tested via qPCR. Interestingly, the chimerism strongly differed in both cohorts as exemplified in **Figure 13a**, showing the percentages of donor derived CD45.1+ white blood cells (WBC) from week eight post transplantation. The relative number of CD45.1 donor cells remained stable in the first cohort; however, in the second cohort the CD45.1 population decreased (e.g. in the WBC from ~12 % to ~8 %). The percentages of CD45.1+ WBC between the nt vector and the gene KO were not significantly different within either of the cohorts, irrespective of the repopulation capacities (**Figure 13b and c**). Notably, in the first cohort a high degree of heterogeneity in the repopulation capacities of all CD45.1+ populations, particularly in the KO group, was observed. Due to the small sample size and high variability, data only from the first cohort is not informative.

In addition to the total WBC, the major hematopoietic subsets were analyzed. B cells form more than 50 % of the total WBCs and showed similar dynamics as the WBCs (**Figure 13d and e)**. Since Evi2a is not expressed in B cells, the KO and nt vector showed similar repopulation capacities as expected. Other than in the B cells, a decrease in the donor myeloid compartment was expected, considering that Evi2a is highly expressed in monocytes. However, the data suggests no effect of the KO on myeloid differentiation in either of the cohorts (**Figure 13f and g**). The last population sorted are CD45.1+ T cells, which also do not significantly increase or decrease upon Evi2a deletion. This population, however, shows a high degree of heterogeneity, even in the second cohort (**Figure 13h and i**). Out of the donor cells, the degree to which the individual populations contribute to the total WBC is plotted in **Figure 13j-l.** The four-, eight-

and twelve-week timepoints after transplantation are visualized, whereas for the latter, only data from the first cohort is represented. As in the previous analysis (**Figure 13a-i**), the KO did not show a significant influence on the contribution of the individual subsets on the total WBCs. However, at eight weeks post-transplant myeloid cells seemed to be slightly upregulated, and T cells downregulated in the KO mice (**Figure 13j and k**). This effect was not evident at the twelve weeks timepoint, where only the first cohort has been analyzed. Analysis of the second cohort will still be needed for final conclusions (**Figure 13l**).

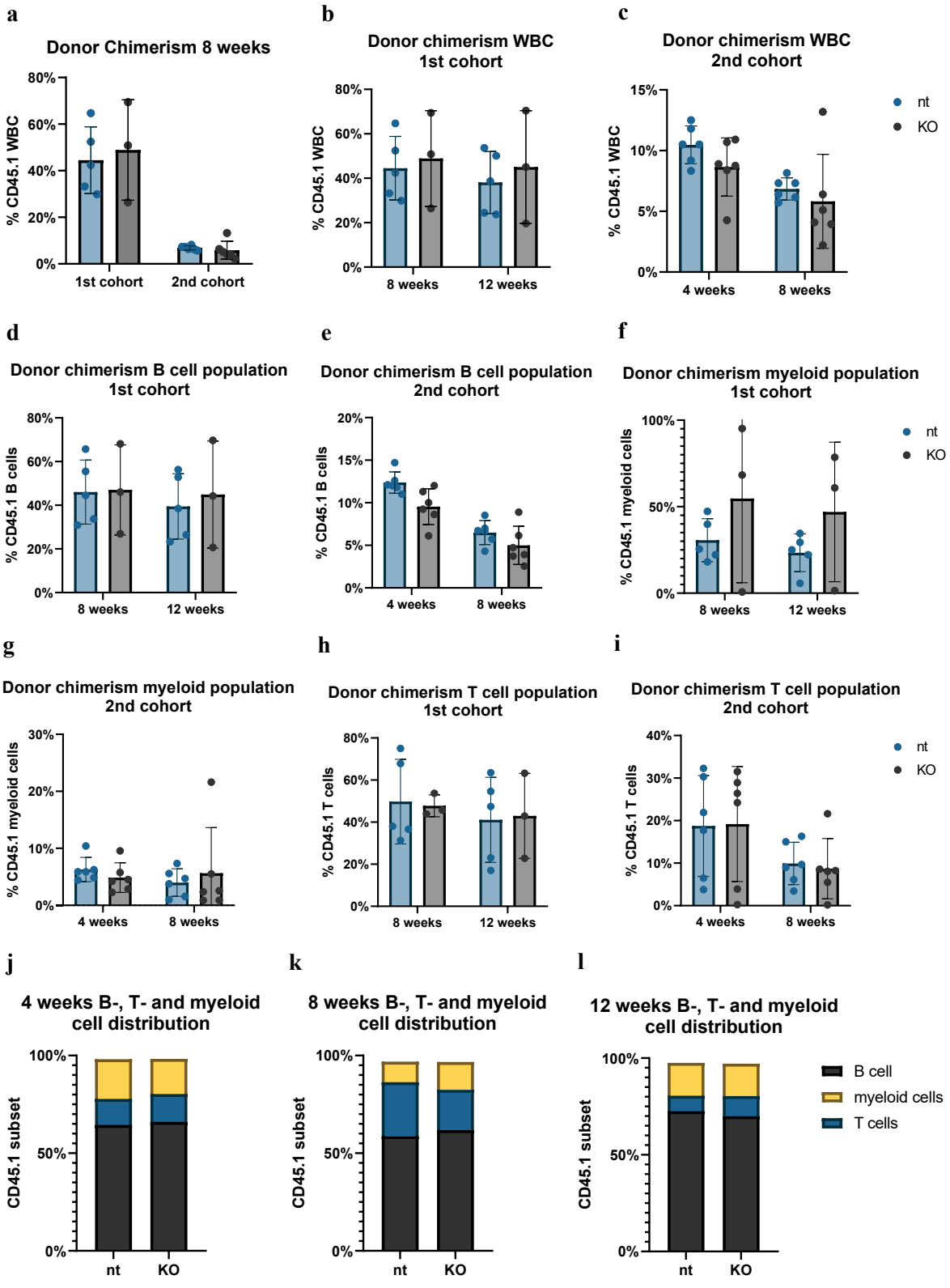
a
Donor Chimerism 8 weeks
% CD45.1 WBC
80%
60%
40%
20%
0%
1st cohort
2nd cohort
b
Donor chimerism WBC
1st cohort
% CD45.1 WBC
80%
60%
40%
20%
0%
8 weeks
12 weeks
c
Donor chimerism WBC
2nd cohort
% CD45.1 WBC
15%
10%
5%
0%
4 weeks
8 weeks
nt
KO
d
Donor chimerism B cell population
1st cohort
% CD45.1 B cells
80%
60%
40%
20%
0%
8 weeks
12 weeks
e
Donor chimerism B cell population
2nd cohort
% CD45.1 B cells
20%
15%
10%
5%
0%
4 weeks
8 weeks
f
Donor chimerism myeloid population
1st cohort
% CD45.1 myeloid cells
100%
50%
0%
8 weeks
12 weeks
nt
KO
g
Donor chimerism myeloid population
2nd cohort
% CD45.1 myeloid cells
30%
20%
10%
0%
4 weeks
8 weeks
h
Donor chimerism T cell population
1st cohort
% CD45.1 T cells
80%
60%
40%
20%
0%
8 weeks
12 weeks
i
Donor chimerism T cell population
2nd cohort
% CD45.1 T cells
40%
30%
20%
10%
0%
4 weeks
8 weeks
nt
KO
j
4 weeks B-, T- and myeloid
cell distribution
CD45.1 subset
100%
50%
0%
nt
KO
k
8 weeks B-, T- and myeloid
cell distribution
CD45.1 subset
100%
50%
0%
nt
KO
l
12 weeks B-, T- and myeloid
cell distribution
CD45.1 subset
100%
50%
0%
nt
KO
B cell
myeloid cells
T cells

Figure 13: Evi2a deletion does not influence peripheral blood cell parameters in comparison to the non-targeting vector a) donor chimerism of transplanted CD45.1+ WBCs show variance between the two cohorts **b)** donor chimerism of CD45.1+ WBC population in the first cohort after 8 and 12 weeks **c)** and the second cohort after 4 and 8 weeks **d)** donor chimerism in the CD45.1+ B cell population in the first cohort after 8 and 12 weeks **e)** and the second cohort after 4 and 8 weeks **f)** donor chimerism in the CD45.1+ myeloid cell population in the first cohort after 8 and 12 week**s g)** and the second cohort after 4 and 8 weeks **h)** donor chimerism in the CD45.1+ T cell population in the first cohort after 8 and 12 weeks **i)** and the second cohort after 4 and 8 weeks **j)** contribution of B cells, T cells and myeloid cells to donor CD45.1 WBC subset of the second cohort at 4 weeks **k)** both cohorts at 8 weeks **l)** and the first cohort at 12 weeks after transplantation

Taken together, the KO donor cells give rise to all three lineages to a comparable extent as in the nt control. Indicating, that the KO of Evi2a has no influence on adult hematopoiesis. Since ~5 % of donor cells contained an unmutated Evi2a gene, we examined whether these WT cells were positively selected over the transduced counterparts and therefore expanding and reconstituting the blood system. The mCherry expression of CD45.1+ cells normalized to CD45.1/2+ cells were ranging from 0 % to up to 60 %. Of note, the mCherry+ population was again assessed via the shift in MFI (normalized to mCherry in untransduced cells), therefore results may be interpreted with caution. In the B cell population (**Figure 14a**) the percent of mCherry is lowest and blow 10 % in most of the mice. In the myeloid cells however, 15 % to 30 % were mCherry+, with very few outliers. Following the hypothesis that Evi2a is involved in myeloid differentiation, a selection for WT clones in the myeloid branch would be expected. This is, however, not supported by the mCherry expression profiles (**Figure 14b**). Lastly, mCherry expression in the KO T cells was highly variable, which can be attributed to the low CD45.1 T cell counts (**Figure 14c**). To overcome the issue of indistinct mCherry peaks, downstream genetic analyses were performed on the sorted T, B, and myeloid cells, to more reliably assess to which extent the KO cells contribute to the CD45.1+ population. The nt control cannot be analyzed by determining the amount of cut DNA by sanger sequencing. Therefore, a qPCR with genomic DNA was performed, measuring Cas9 compared to ApoB as a reference gene. The relative quantification of Cas9 for each cohort at different time points is shown in **Figure 14d-f**. In general, Cas9 decreased with time, consistent with low mCherry expression. Together, these findings indicate a negative selection for transduced blood cells.

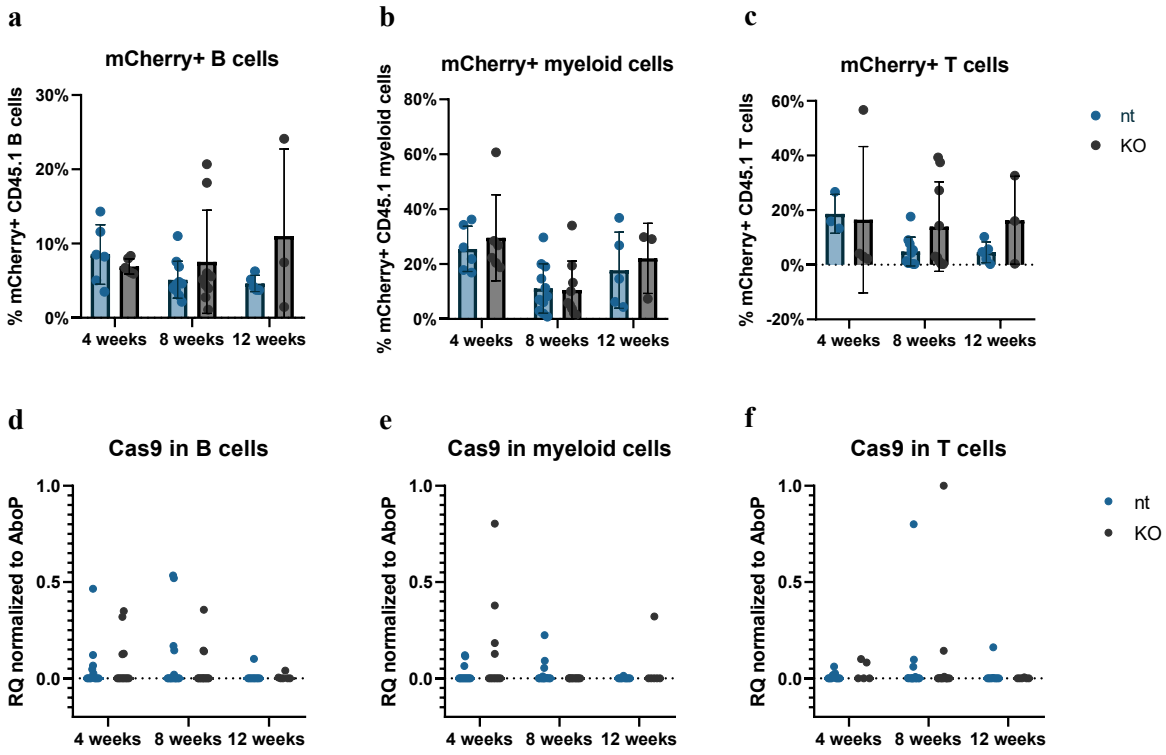

Figure 14: mCherry expression and Cas9 integration in peripheral blood decrease in a timely manner a-c) mCherry espression in donor CD45.1+ population (both cohorts pooled) in **a)** B cells **b)** T cells **c)** myeloid cells is low throughout all time points **d-f)** Cas9 at 4 weeks, 8 weeks and 12 weeks post transplant detected by qPCR and shown as relative quantification normalized to ApoB, while 1 reflects identical copynumbers of ApoB and Cas9 and 0 reflect no Cas9 in CD45.1+ **d)** B cells, **e)** myeloid cells **f)** T cells

3.4 Colony formation potential is not influenced by the KO

To functionally assess the effect of the KO *in vitro*, single cell expansion and colony formation capacities were measured. Two scCFU assays were performed by seeding a single cell into each well of a 96-round well plate. In the first experiment no colonies grew in the nt control, the exact reason for this cannot be assessed in retrospective. Most likely however, technical errors during processing attribute for the lack of expansion. **Figure 15a** shows the number of colonies that grew in the second experiment. The counted colonies were subdivided into big (**Figure 15b**), and medium sized (**Figure 15c)** colonies The number of colonies in both the KO and the nt cells ranges around 20 colonies per plate, compared to 30 colonies per plate in the WT control. So, the transduction process most likely limits the colony formation capacities of LSK cells.

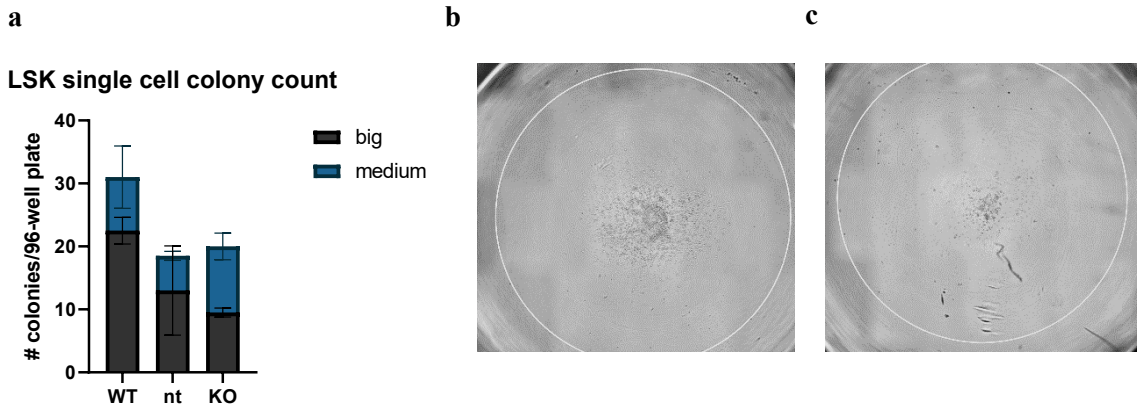

Figure 15: a) Number of colonies in single cell Colony Forming Unit (scCFU) Assay are equally decreased in both transduced groups compared to WT cell **b)** example of big colony **c)** example of medium sized colony

4 Discussion

The previously shown relevance of Evi2a in embryogenesis has proven to be limited to early developmental stages. A KO of Evi2a did not lead to competitive advantages or disadvantages in cell growth, as shown *in vitro* by co-cultivation of transduced murine AML cells with untransduced cells. Also, there was no detectable difference in the reconstitution of B, T, or myeloid cells in peripheral blood within the first twelve weeks after transplantation of Evi2a KO LSK cells compared to LSK cells transduced with the nt vector. Although Evi2a did not prove to significantly influence hematopoiesis, we were able to establish a robust protocol to KO Evi2a in cell lines and LSK cells. Establishing a novel method comes along with many particularities, starting from developing the construct, to validation and finally functionally applying the protocol *in vivo*.

4.1 Production of the lentiviral CRISPR/Cas9 system carrying the gRNAs was successful

To induce targeted genetic KO in stem cells, CRISPR/Cas9 has progressed to be the method of choice. However, to deliver the CRISPR/Cas9 different systems can be applied [24]. According to *Lattanzi et al. (2019),* electroporation has proven to induce the highest genome-editing efficiency while keeping toxicity low [25]. However, electroporation tests in our lab, failed in successfully transducing stem cells via RNP delivery. Therefore, we decided to use an alternative system, based on viral transduction.

The transduction system has to fulfill several requirements. First, we wanted to knock-out stem cells that should maintain stemness while being cultured. Second, we want to select for successfully gene edited cells via an incorporated marker. Third, the maximum number of Cas9 expressing cells should be gene-edited. Forth, the system should enable KO cells to be subsequently monitored *in vivo*. And at last, toxicity has to be avoided to keep the initial number of mice sacrificed for LSK isolation small. For the KO system, this means that no system should be employed where cells require cycling, excluding the application of gamma-retroviruses. Further, a marker for selection has to be included in the construct that ensures quick and unharmful selection. Lentiviral transduction was therefore the method choice.

4.2 Genetic lesions are evident in all tested cells

4.2.1 CRISPR/Cas9 gRNA delivery is effective in NIH3T3 cells

When transducing NIH3T3 cells, low titers did not negatively influence the survival of the cells. The low titers were used in these cell lines, since virus production was not fully optimized and repeating the experiment would not have improved to quality of following experiment on AML cell lines or LSK cells. Interestingly, 7 days after sorting only ~90 % of the sorted cells were mCherry+, whereas 13 days later the mCherry+ proportion increased. When sequencing at d0 the DNA cutting efficiency was still low (i.e. ~25 % with guide 1 and ~70 % with guide 2), at day 7 however, only ~10 % of the cells transduced with guide 2 still had uncut DNA. The later observed increase suggests that transduced cells either have an advantage, or that the Cas9 integration is still ongoing to up to 20 days post transduction.

4.2.2 KO introduction in MLLAF9$^{FLT3(ITD)}$ and MLLAF9^{ctrl} cells is less effective and no *in vitro* functional effect is evident

In the MLLAF9 cells initially major errors were observed. The cells were successfully transduced, however one day after sorting, all the cells died, and high degrees of degranulation were evident (initially misinterpreted as bacterial infections). After several failed transductions, we consulted Steve Sykes and found out that the problem was cooling the cells to 4 °C when sorting. The experiment was repeated using VB3 and VB6 without any cooling, and indeed, less cell death was observed after sorting. Having viable and transduced cells, this enabled us to perform a co-culture assay. Since both, the nt control and Evi2a KO cells, have a competitive disadvantage to WT cells, the growth inhibition is more likely caused by stress due to the transduction regime or the lentiviral insert, rather than the KO of Evi2a. The 100 % mCherry+ control wells also show a significant decrease of mCherry expression. This reduction could be caused by untransduced cells, that fell into the mCherry+ gate while sorting. Another reason for the loss of mCherry+ cells could also be due to promotor silencing, however the increase in genetic lesions while downregulation of mCherry expression is counterintuitive, since mCherry and Cas9 are under control of the same promotor. Alternatively, it is also possible that the fluorescence intensity decreases upon cultivation, but cells might maintain the KO to an

unknown degree. The latter is supported by sequencing data from day 7 and day 14 (**Figure 11f**), since the proportions of intact Evi2a sequences further decreased to nearly 0 %. Dynamics of mCherry intensities upon long term cultivation should be further studied. To interrogate the cause for the decrease in mCherry expression, a co-culture experiment could be repeated, whereas the Evi2a loci are sequenced in additions to analysis by flow cytometry.

4.2.3 mCherry expression is lower in transduced LSK cells

Next, a pilot transduction in the LSK cells was set up. In this run a very mild increase in the MFI was observed, as expected, since transduction of primary cells is usually lower. However, also a difference in the MFI of the KO and the nt vector was evident which was observed in all re-sorting experiments and is exemplified in **Figure 12a**. This could have several reasons. The gRNA in the plasmid could negatively affect the cells, leading to a selection for lower expressing cells. Other, more technical restraints could lead to the shift, such as different toxicities in the viral supernatants or slight inaccuracies in titration that would lead to varying virus concentrations. Because of varying MFIs in both transduced groups, and the slight shift in general the gating strategy based on a defined positive population was not applicable, as done in the MLLAF9 and NIH3T3 cells. To provide ideal gating for the sort, quartiles of the top 10 %, 2nd 10 %, 3rd 10 % and 4th 10 % were sorted and sent in for sanger sequencing. KO efficiencies were above 25 % in the 1st, 2nd, and 3rd 10 % (assessed by sanger sequencing, data not shown). Considering practicality and mouse numbers, the top 30 % were sorted for further experiments and the final transplantation. In retrospective, a co-transfection approach with 2 gRNAs would have been more effective in achieving higher transduction ratios, as shown by *Lattanzi et al. (2019)* [25]. Whether higher Cas9 expression also leads to a better or more robust KO remains to be evaluated.

4.3 Transplanted KO LSK cohorts expanded to different degrees during *in vitro* transduction

Cultivation of HSCs unavoidably leads to a certain degree of differentiation, depending on culture conditions [2]. At best asymmetric division of HSCs *in vitro* can be assumed upon proliferation [26]. Consequently, if the cells double, approximately half of the cells will have

differentiated into more mature progenitors. In addition to that, LSK cells consist of only about 10 % HSCs with the remaining cells being progenitors [2]. Although cultivation of LSK cells is not extensively studied, it can be assumed that differentiation into more mature subsets is similar or increased compared to HSCs. Assuming asymmetric division, even in LSK cells, the following scenario is that the isolated and cultivated LSK cells from the first and the second cohort would bias the transplantation.

In the first cohort, 2 x 10^6 LSK cells were initially isolated and transduced. The top 30 % mCherry+ cells were sorted on d3 for transplantation. However, that only summed up to approximately 2 x 10^5 cells, meaning, the cells did not proliferate in culture, and some were lost upon processing. Since 5 x 10^5 cells would have been assumed an actual reduction by 2.5-fold was observed. In the second cohort only 5 x 10^5 cells could be isolated for transduction. Again, the top 30 % mCherry+ cells were sorted on d3, surprisingly this time 3 x 10^5 cells were sorted. Consequently, the cells expanded by 2-fold *in vitro*. Considering the above made assumptions on *in vitro* differentiation of stem cells, in the first cohort all transplanted cells were undifferentiated and are therefore LSK equivalents. In the second cohort, however, half of the transplanted cells have probably differentiated to some degree and only half of the transplanted cells would be LSK equivalents. Transplantation of half of the LSK equivalents in the second cohort compared to the first cohort would explain the lower doner chimerism. The reason for the difference in *ex vivo* expansion, however, is in question. Technically, the only difference, was that second cohort was directly seeded onto retronectin-coated plates, which has been shown in our lab to improve stem cell viability and retain stemness.
Furthermore, these assumptions do not take possible selections of the transduction for more differentiated cells into account and are solely based on hypothetical scenarios. Yet, the lower doner chimerism observed in the second cohort indicates a difference in the transplanted cell populations.

4.3.1 Donor chimerism is not altered in the KO compared to the nt control because WT CD54.1+ LSK cells expand

The peripheral blood was FACS sorted and analyzed for donor CD45.1+ WBCs. As mentioned above the donor chimerism in the first cohort is significantly higher, than in the second cohort might be due to the number of LSK equivalents transplanted. Besides that, the decrease in donor chimerism from the four to the eight weeks timepoint in the second cohort is quite unexpected. Since the decrease is observed in both, KO and nt, the effect is likely to be caused by a general impairment of the cells upon *in vitro* transduction. The same effect is not present in the first cohort. Yet the high variability potentially falsifies the data or does not allow visualization of chimerism kinetics. In the first cohort, several technical constraints appeared that would suggest excluding the data from the analysis. Most importantly, the transplantation was possibly flawed since it was the first ever experimental i.v. injection performed by Theo Aurich. Due to lack of experience and routine, some drops of the cell suspension might not have been properly injected in the KO group, e.g. going paravenous into the tail tissue, meaning less cells were transplanted. Since that the first cohort might be invalid due to flawed transplantation, interpreting the data from the second cohort would only suggest no effect of an Evi2a KO on repopulation dynamics within the first eight weeks after transplantation. Although, the KO LSKs seem to have a slightly decreased repopulation capacity compared to the nt. Both, mCherry expression data and the qPCR, show that the donor CD45.1 cells do not bear a gene KO or the nt vector. The reason for absence of Cas9 carrying cells in the peripheral blood is not fully clear. Most likely the co-transplanted WT cells that could not be avoided while sorting for mCherry+ cells took over due to some sort of competitive advantage over transduced cells. The *in vitro* data on AML cells and the scCFU assay, suggest the latter to be true, since a growth disadvantage was observed in both transduced groups, independent on whether the cells carry a KO or not.

To overcome this problem, remaining WT cells should be avoided in the transplantation setting, for instance by knocking-out Evi2a, or any gene of interest, using a co-transfection system could be applied [27]. Alternatively, electroporation might be reconsidered, since higher DNA cutting efficiencies were observed [25]. *Gundry et al*. (2016) also reported high efficiencies with sgRNA in Cas9 expressing mice, reporting efficiencies of 67 % [28] as opposed to the hardly distinguishable transduced population in the applied protocol.

4.4 Colony formation potential is not influenced by the KO

A similar phenomenon was observed in the scCFU assay, in which both had reduced capacities to give rise to viable colonies. In this assay it has to be noted that usually long-term HSCs would be seeded instead of LSK cells. A possible flaw of the experiment is certainly the decreased colony forming capacity of LSK cells compared to the multipotent long-term-HSCs. The comparatively low number of colonies that grew are more prone to random fluctuations and culture conditions effecting the cell growth. To validate the scCFU assay, it would be beneficial to repeat the setup with more replicates and to assess on whether the colonies that expanded are transduced or WT clones.

5 Conclusion

Taken together, a true effect of Evi2a in adult hematopoiesis and AML is not supported by the performed experiments. However, an effect can still not be fully ruled out since experimental groups were comparatively small and the variability within the groups is high. Furthermore, the transplanted cells do not show Cas9 integration and have low or no mCherry expression, suggesting an expansion of WT cells, which makes assumptions about the KO effect impossible. Besides that, if the effect was marginal, it cannot be detected in a competitive transplantation assay since supportive donor cells or remaining recipients might compensate for a loss-of-function in the KO cells.

Nonetheless, we were able to establish a basis for transplanting KO LSK cells into recipient mice. Notably, the protocol must be optimized to avoid co-transplantation of WT cells that could possibly take over *in vivo*. Possible optimization could be done, by introducing two gRNA to increase the KO efficiency, to sort the transduced population more conservatively, or to change the fluorescent protein in the vector to enable a clearer distinction of the transduced LSK cells.

Bibliography

[1] M. A. Rieger and T. Schroeder, "Hematopoiesis," *Cold Spring Harb Perspect Biol,* no. 4, 2012.

[2] L. E. Puton and D. T. Scadden, "Limiting Factors in Murine Hematopoietic Stem Cell Assays," *Cell Stem Cell,* no. 1, pp. 263-270, 2007.

[3] E. Laurenti and B. Göttgens, "From Haematopoietic stem cells to complex differentiation landscapes," *Nature,* no. 553, pp. 418-426, 2018.

[4] H. Cheng, Z. Zheng and T. Cheng, "New paradigms on the hematopoietic stem cell differentiation," *Protein Cell,* vol. 11, no. 1, pp. 34-44, 2020.

[5] M. Brand and E. Morrissey, "Single Cell Fate Decisions of Bipotential Hematopoietic Progenitors," *Curr Opin Hematol.,* vol. 27, no. 4, pp. 232-240, 2020.

[6] J. N. Pucella, S. Upadhaya and B. Reizis, "The Source and Dynamics of Adult Hematopoiesis: Insight from Lineage Tracing," *Annual Review of Cell and Developmental Biology,* no. 36, pp. 529-550, 2020.

[7] A. Czechowicz, R. Palchaudhuri, A. Scheck, Y. Hu, J. Hoggatt, B. Saez, W. W. Pang, M. K. Mansour, T. Tate, Y. Y. Chan, E. Walck, G. Wernig, J. a. Shizuru, F. Winau, D. T. Scadden and D. J. Rossi, "Selective hematopoietic stem cell ablation using CD117-antibody-drug-conjugates enables safe and effective transplantation with immunity preservation," *Nature Communications,* vol. 10, no. 1, 2019.

[8] B. Dykstra, D. Kent, M. Bowie, L. McCaffrey, M. Hamilton, K. Lyones, S.-J. Lee, R. Brinkman and C. Eaves, "Long-Term Propagation of Distinct Hematopoietic Programs In Vivo," *Cell Stem Cell,* no. 1, pp. 218-229, 2007.

[9] F. Dong, S. Hao, S. Zhang, C. Zhu, H. Cheng, Z. Yang, F. K. Hamey, X. Wang, A. Gao, F. Wang, Y. Gao, J. Dong, C. Wang, J. Wang, Y. Lan, B. Liu, H. Ema, F. Tang, B. Göttgens, P. Zhu and T. Cheng, "Differentiation of transplanted haematopoietic stem cells tracked by single-cell transcriptomic analysis," *Nature Cell Biology,* no. 22, pp. 630-639, 2022.

[10] A. M. Buchberg, H. G. Bedigian, N. A. Jenkins and N. G. Copeland, "Evi2a, a Common Integration Site Involved in Murine Myeloid Leukemogenesis," *Molecular and Cellular Biology,* vol. 10, no. 9, pp. 4658-4666, 1990.

[11] H. Döhner, D. J. Weisdorf and C. D. Bloomfield, "Acute Myeloid Leukemia," *The New Englang Journal of Medicine,* vol. 373, no. 12, pp. 1136-1152, 2015.

[12] J. N. Saultz and R. Garzon, "Acute Myeloid Leukemia: A Concise Review," *Journal of Clinical Medicine,* vol. 5, no. 33, 2016.

[13] L. F. Newell and R. J. Cook, "Advances in acute myeloid leukemia," *BMJ,* no. 375, 2021.

[14] cytiva, *Ficoll-Paque PREMIUM density,* 2020.

[15] H.-J. Lee, Y.-S. Lee, H.-S. Kim, Y.-K. Kim, J.-H. Kim, S.-H. Jeon, S. Kim, H. Miyoshi, H.-M. Chung and D.-K. Kim, "Retronectin enhances lentivirus-mediated gene delivery into hematopoietic progenitor cells," *Biologicals,* vol. 37, no. 4, pp. 203-209, 2009.

[16] O. Shalem, N. E. Sanjana, E. Hartenian, X. Shi, D. A. Scott, T. Mikkelson, D. Heckl, B. L. Ebert, D. E. Root, J. G. Doench and F. Zhang, "Genome-scale CRISPR-Cas9 knowckout screening in human cells," *Science,* no. 343, pp. 84-87, 2014.

[17] N. E. Sanjana, O. Shalem and F. Zhang, "Improved lentiviral vectors and genome-wide libraries for CRISPR screening.," *Nature Methods,* no. 11, pp. 783-784, 2014.

[18] A. Smogorzewska , *Addgene plasmid # 99154.*

[19] S. Filomena, L. Passarinha, F. Sousa, J. A. Queiroz and F. C. Domingues, "Influence of Growth Conditions on Plasmid DNA Production," *J. Microbiol. Biotechnol.,* vol. 19, no. 11, p. 1408–1414, 2009.

[20] K. J. Livak and T. D. Schmittgen, "Analysis of Relative Gene Expression Data Using Real-Time Quantitative PCR and 2-(delat-delta-Ct) Method," *Methods,* vol. 25, no. 4, pp. 402-408, 2001.

[21] K. J. Carroll, C. A. Makarewich, J. McAnally, D. M. Anderson, L. Zentilin, N. Liu, M. Giacca, R. Bassel-Duby and E. N. Olson, "A mouse model for adult cardiac-specific gene deletion with CRISPR/Cas9," *PNAS,* vol. 113, no. 2, pp. 338-343, 2016.

[22] P. Govey, M, Y. Zhang and H. J. Donahue, "Murine-specific primers used for real-time RT-PCR for relative quantification of donor cell DNA.," *PLOS ONE,* 2016.

[23] P. Lin, D. Correa, Y. Lin and A. I. Caplan, "Polybrene Inhibits Human Mesenchymal Stem CellProliferation during Lentiviral Transduction," *PLoS ONE,* vol. 6, no. 8, 2011.

[24] Z. Zhang, Y. Zhang, F. Gao, S. Han, K. S. Cheah, H.-F. Tse and Q. Lian, "CRISPR/Cas9 Genome-Editing System in Human Stem Cells: Current Status and Future Prospects," *Molecular Therapy Nucleic Acids,* vol. 9, 2017.

[25] A. Lattanzi, V. Meneghini, G. Pavani, F. Amor, S. Ramadier, T. Felix, C. Antoniani, C. Masson, O. Alibeu, C. Lee, M. H. Porteus, G. Bao, M. Amendola, F. Mavilio and A. Miccio, "Optimization of CRISPR/Cas9 Delivery to Human Heamtopoietic Stem and Progenitor Cells for Therapeutic Genomic Rearrangements," *Molecular Therapy,* vol. 27, no. 1, pp. 137-150, 2019.

[26] A. C. Wilkinson and H. Nakauchi, "Stabalizing heamtpoietic stem cells in vitro," *Curr Opin Genet Dev.,* no. 64, pp. 1-5, 2020.

[27] M. Mandl, H. Ritthammer, A. Ejaz, S. A. Wagner, F. M. Hatzmann, S. Baumgarten, H. P. Viertler, M. E. Zwierzina, M. Mattesich, V. Schiller, T. Rauchenwald, C. Ploner, P.

Waldegger, G. Pierer and W. Zwerschke, "CRISPR/Cas9-mediated gene knockout in human," *ADIPOCYTE,* vol. 9, no. 1, pp. 626-635, 2020.

[28] M. C. Gundry, L. Brunetti, A. Lin, A. E. Mayle, A. Kitano, D. Wagner, J. I. Hsu, K. A. Hoegenauer, C. M. Rooney, M. A. Goodell and D. Nakada, "Highly Efficient Genome Editing of Murine and Human Hematopoietic Progenitor Cells by CRISPR/Cas9," *Cell Reports,* no. 17, pp. 1453-1461, 2016.

[29] Z. Bao, Y. Huang, J. Chen, Z. Wang, J. Qian, J. Xu and Y. Zhao, "Validation of Reference Genes for Gene Expression Normalization in RAW264.7 Cells under Different Conditions," *Biomed Res Int,* vol. 2019, 2019.

[30] A. K. Shanmugam, B. A. Mysona, J. Wang, J. Zhao, A. Tawfik, A. Sanders, S. Markand, E. Zorrilla, V. Ganapathy, K. E. Bollinger and S. B. Smith, "Progesterone receptor membrane component 1 (PGRMC1) expression in murine retina," *Curr Eye Res,* vol. 41, no. 8, pp. 1105-1112, 2016.

List of Figures

List of Tables

List of Equations